frontiers | Frontiers in Marine Science

TYPE Original Research
PUBLISHED 04 January 2023
DOI 10.3389/fmars.2022.1003321

OPEN ACCESS

EDITED BY
Sara Fratini,
University of Florence, Italy

REVIEWED BY
Hsi-Te Shih,
National Chung Hsing University, Taiwan
Bert W. Hoeksema,
Naturalis Biodiversity Center, Netherlands

*CORRESPONDENCE
Benny K. K. Chan
chankk@gate.sinica.edu.tw

SPECIALTY SECTION
This article was submitted to Marine Evolutionary Biology, Biogeography and Species Diversity, a section of the journal Frontiers in Marine Science

RECEIVED 26 July 2022
ACCEPTED 13 October 2022
PUBLISHED 04 January 2023

CITATION
Wong KJH, Tsao Y-F, Qiu J-W and Chan BKK (2023) Diversity of coral-associated pit crabs (Crustacea: Decapoda: Cryptochiridae) from Hong Kong, with description of two new species of *Lithoscaptus* A. Milne-Edwards, 1862.
Front. Mar. Sci. 9:1003321.
doi: 10.3389/fmars.2022.1003321

Diversity of coral-associated pit crabs (Crustacea: Decapoda: Cryptochiridae) from Hong Kong, with description of two new species of *Lithoscaptus* A. Milne-Edwards, 1862

Kingsley J. H. Wong [1,2], Yao-Feng Tsao [1], Jian-Wen Qiu [3] and Benny K. K. Chan [1*]

[1]Biodiversity Research Center, Academia Sinica, Taipei, Taiwan, [2]Institute of Ecology and Evolutionary Biology, National Taiwan University, Taipei, Taiwan, [3]Department of Biology, Hong Kong Baptist University, Hong Kong, Hong Kong SAR, China

Highly specialized cryptochirid crabs are obligate symbionts of scleractinian corals in tropical and subtropical seas. General morphologies of cryptochirid crabs remain poorly described due to their small size and difficulties in collection; thus, the current inventory is probably an underestimation. In the present study, we sampled cryptochirid crabs from coral communities in Hong Kong. In the literature, only *Cryptochirus hongkongensis* (now *Neotroglocarcinus hongkongensis*) with unknown hosts had been recorded in Hong Kong since 1936. In addition to morphological examination, identification in the present study is further supported by sequence divergence of mitochondrial cytochrome c oxidase I (COI) and 16S ribosomal DNA markers. Six operative taxonomic units (OTUs), representing four species and one species complex with two species, were revealed among our material: *Cryptochirus coralliodytes*, *Lithoscaptus paradoxus*, *Lithoscaptus doughnut* sp. nov., *Lithoscaptus scottae* sp. nov., and *Xynomaia sheni* species complex. Morphological description of these species is provided, including description of the two new pseudocryptic species. The hosts of the genus *Lithoscaptus* belong largely to the Merulinidae, while *L. doughnut* sp. nov. inhabits the Plesiastreidae.

KEYWORDS

gall crabs, coral associates, scleractinian coral, biodiversity, West Pacific

Introduction

Coral reef ecosystems are highly productive, harboring remarkable species diversity (Crossland et al., 1991; Reaka-Kudla, 1997). Recent estimates on species associated with coral reefs range from 550,000 to 1,330,000 (Fisher et al., 2015), and over 91% of such species remain to be described (Mora et al., 2011). Decapod crustaceans are an important component of the tropical reef fauna (Castro, 1976; Ross, 1983), among which several brachyuran lineages, including the Cryptochiroidea and Trapezoidea (Domeciidae, Tetraliidae and Trapeziidae), and numerous xanthioid (e.g., *Cymo*) and pilumnoid (*Tanaocheles*) species (Castro, 2015), are symbiotic with scleractinian corals. While some of these lineages are "facultative symbionts" (Castro, 1976), none are as specialized as the Cryptochiridae with mature females have pleon modified as an inflated, egg-carrying pouch, with a size comparable to the rest of the individual, often sedentary in domiciles on the surface of scleractinian corals, and sacrificing mobility for physical protection and reproductive success (Vehof et al., 2014). This highly specialized niche is comparable to those of pea crabs of the family Pinnotheridae, which were found to show obligate associations with hosts including edible bivalves and gastropods, and ascidians, holothurians, and echinoids (see De Gier and Becker, 2020).

Members of Cryptochiridae are often referred to as "gall crabs." However, the form of domicile differs substantially within the family. One form inhabits branching corals of the Pocilliporidae, which induces development of an enclosed chamber of two hemispheres of host tissue (e.g., Potts, 1915; Hiro, 1937). Others settle on the surface of massive corals during the megalopa stage, inhibiting the growth of coral polyp at that spot, and from there, they excavate pits or channels of various forms, often leaving a shallow depression around the opening (Hiro, 1937; Simon-Blencher and Achituv, 1997). These two forms exhibit distinct feeding mechanisms (Abelson et al., 1991). Following the definition of galls in plants (Fernandes et al., 2011), typical domiciles induced by *Hapalocarcinus* can be recognized as true galls (thus "gall crabs"). As elaborated by Abelson et al. (1991), the term "pit crabs" might be more appropriate for those pit excavators living especially in massive corals. The several species herein reported from Hong Kong can be referred to as "pit crabs," and we refrain from referring cryptochirids exclusively as "gall crabs." However, given the considerable diversity of cryptochirid domiciles, such as those lodged between septa of mushroom coral of the Fungiidae (Hoeksema et al., 2012; van der Meij et al., 2015), and some forming a canopy-like structure, partially sheltering the opening in hosts of the Agariciidae (Hoeksema et al., 2017; García-Hernández et al., 2020), further definition of common names of cryptochirid crabs based on their domicile morphology may require further investigations.

Cryptic species (morphologically indistinguishable) and pseudocryptic species (minor morphological difference) are biologically distinct species that are erroneously classified (thus hidden) under one species name (Bickford et al., 2007; Lajus et al., 2015), and various cryptochirid lineages may contain previously unrecognized, cryptic diversity. In an alternative understanding, cryptochirids can be "cryptic" for being small in size, well camouflaged, and inhabiting poorly surveyed habitats, thus difficult to sample (see Hoeksema, 2017). In the immensely species-rich region of the Indo-West Pacific, investigation of cryptochirid diversity remains fragmented, despite the discovery of numerous new taxa on hosts previously unreported in the past decade (e.g., van der Meij, 2014; van der Meij, 2015a; van der Meij, 2015b; van der Meij, 2017). In Hong Kong, *Cryptochirus hongkongensis* (now *Neotroglocarcinus hongkongensis*) had been the only species of the Cryptochiridae known prior to this study, then described without reporting on its host (Shen, 1936). Van der Meij (2012) added a tentative record of *Pseudocryptochirus viridis* based on an image showing a domicile opening in a guidebook on the corals of Hong Kong (Scott, 1984). In this paper, we describe the cryptochirid fauna of Hong Kong, comprising of at least five species of pit crabs unrecorded in the literature, including two new pseudocryptic species of *Lithoscaptus*. This study is part of a study aiming to understand the diversity and biogeography of cryptochirids and host relations of coral-associated fauna.

Materials and methods

Surveyed sites, specimen collection, and morphological examination

Hong Kong is located along the northern limit of the Tropics in the Northern Hemisphere, east of the Pearl River outlet (Zhujiang). Given the massive freshwater runoff of some 300 billion m^3 discharged seasonally, territorial seas of Hong Kong comprises of a west-to-east decreasing gradient of fluvial influences, reaching full oceanic conditions in the eastern seas (see Morton et al., 1996). This heterogeneity contributes to diversity of marine habitats and thus inhabited species. Under these conditions, scleractinian corals occur in eastern and northeastern waters as communities on substrates, and a total of 84 species is found in the territorial seas (Chan et al., 2005). Since rehabilitation from severe coastal pollution and disastrous habitat degradation (Morton, 1989; Scott and Cope, 1990), for the past two decades, natural recovery appears limited and difficult (KT Wong et al., 2018; Yeung et al., 2021a), while the process is anticipated to persist in extended time periods (Goodkin et al., 2011).

Six shallow-water sites, all of considerable scleractinian coverage (Yeung et al., 2021a), were surveyed from 2012 to 2019, during the implementation of coral bioerosion and coral bleaching projects (Xie et al., 2016; Yeung et al., 2021b; Zhang et al., 2022). Five of these sites were near Sai Kung, and one in

Mirs Bay, northeast of the territory, and locations of these sites are shown in Figure 1. In general, coral coverage of these sites was distributed from the intertidal zone to depths <5 m, dominated by stress-tolerant scleractinian species, such as those belonging to the genera *Psammocora*, *Pavona*, *Favites*, and *Platygyra*, while the below the deeper reef zone, there were sandy or gritty bottoms of poor visibility.

Domicile openings of cryptochirids, as shown in Figures 2–4, were visually searched underwater during SCUBA diving. These openings were not analyzed in several previous studies of coral borer, such as dumbbell-shaped openings created by *Lithophaga* mussels and the circular ones created by *Spirobranchus tetraceros* (Xie et al., 2016), and colony surfaces immediately around openings were observed to suffer from lesions and prone to diseases (KT Wong et al., 2015). Domicile openings and host corals were photographed *in situ*. The inhabiting crabs, along with the domicile and small fragments of the host, were retrieved and preserved in 95% ethanol. Sampled crabs (Figure 5) were examined under a stereomicroscope (Olympus SZX7) and preliminarily sorted based on morphological characters presented in taxonomic works (Fize and Serène, 1957; Kropp, 1988a; Kropp, 1990). Line drawings were drawn based on structures photographed under a digital camera (Panasonic DM C-GH4). For collected crabs, taxonomic schemes, measurements, and morphological terminology follow those of Kropp (1990) and Davie et al. (2015). Abbreviations CW, CL, Mxl, Mxp, P, Plp, and G, respectively, represents carapace width and length, maxilla (1 and 2), maxilliped (1–3), pereiopod (1–5), female pleopod (1–3), and male gonopod (1 and 2). Host corals were identified from *in situ* photographs and retrieved fragments based on works of Scott (1984); Chan et al. (2005), and Dai and Cheng (2020). Images of preserved material are printed in monochrome. The material examined in this study was deposited into the collections of the Biodiversity Research Museum, Academia Sinica (ASIZCR) and Coastal Ecology Laboratory (CEL), Biodiversity Center, Academia Sinica, Taipei, and Swire Institute of Marine Science, the University of Hong Kong, Hong Kong (SWIMS). For all taxa mentioned in the text, the authority and year of original publication are enumerated in Appendix 1, and full references are not provided for simplicity.

Molecular analysis

Total genomic DNA was extracted from eggs of females, or pereiopod 5 of male crab specimens by using DNeasy ® Blood and Tissue Kit (Qiagen, CA, USA) according to instructions provided by the manufacturer. Partial sequences of two mitochondrial DNA markers (COI and 16S rDNA) were amplified following the protocol from previous studies: those of COI using primers LCO1490 and HC02198 (Folmer et al., 1994; Feller et al., 2013) and of 16S rDNA using 1471 and 1472 (Crandall and Fitzpatrick, 1996). Polymerase chain reactions (PCRs) were conducted in DNA Engine Thermal Cycler (Bio-Rad, Richmond, CA, USA), and the products were checked by electrophoresis on 1.5% agarose gel in 1× TAE buffer. DNA purification and Sanger DNA sequencing were performed by Genomics BioSci and Tech Ltd. (New Taipei City, Taiwan). The sequences were assembled and edited in Geneious 7.0.6 (https://www.geneious.com).

FIGURE 1
Map showing surveyed sites in Hong Kong.

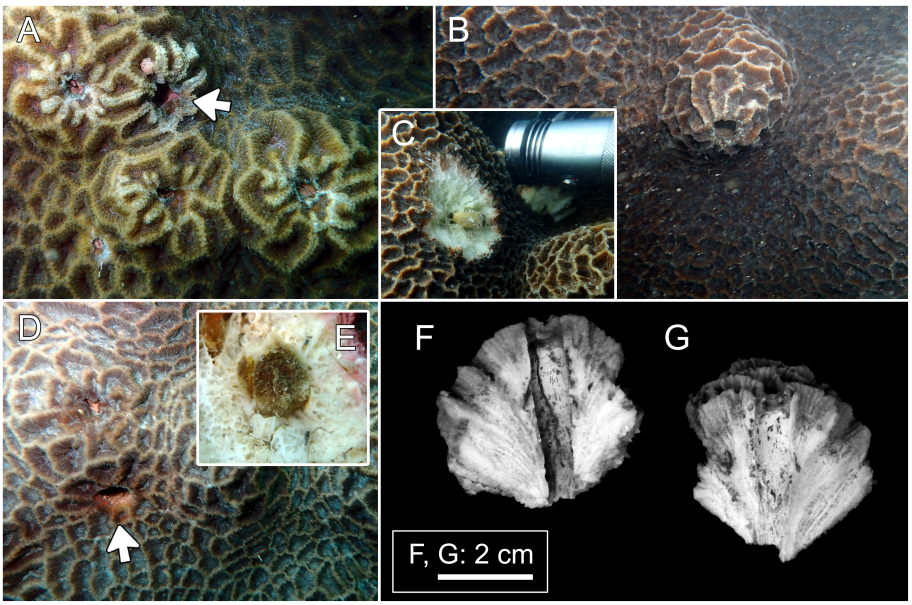

FIGURE 2
Host and domicile of *Lithoscaptus paradoxus*. **(A)** *Platygyra contorta*, Long Ke Tsai; **(B, C)** *P. acuta*, Tai She Wan; **(D, E)**, *P. acuta*, Long Ke Tsai. Insets **(C, E)** showing retrieved crabs. Arrows in panels **(A, D)** showing openings of domiciles. Cross-section of domicile: **(F, G)** Bluff Island.

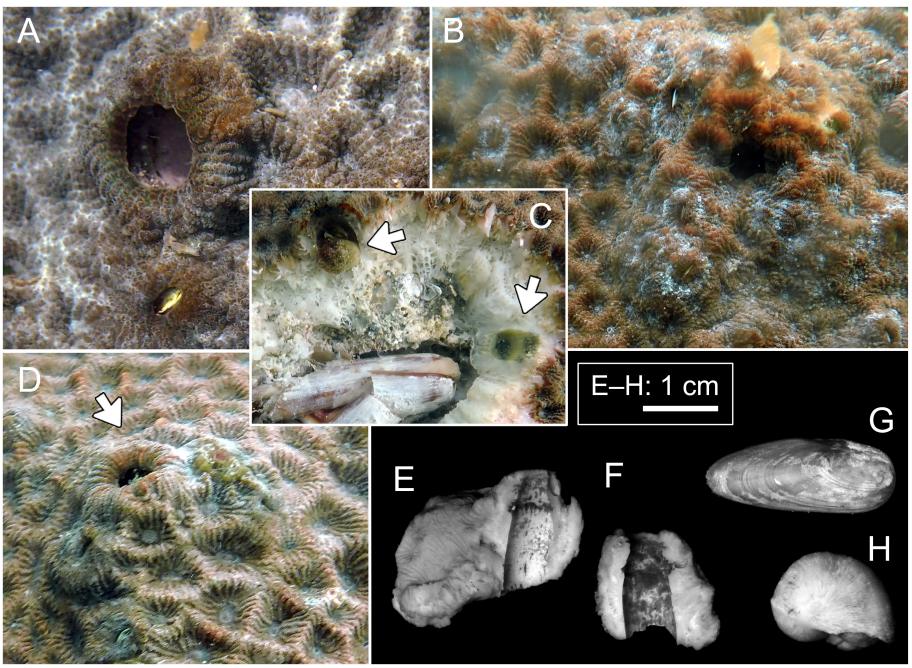

FIGURE 3
Host and domicile of *Lithoscaptus scottae* sp. nov. **(A–D)** *Coelastrea aspera*, Pak Lap Tsai. Arrows in panel **(C)** showing two retrieved crabs; arrow in panel **(D)** showing opening of domicile. Cross-section of domicile: **(E, F)** Pak Lap Tsai. Boring mollusks found within the same colony of *C. aspera*: **(G)** *Lithophaga* sp.; **(H)** *Leptoconchus* sp.

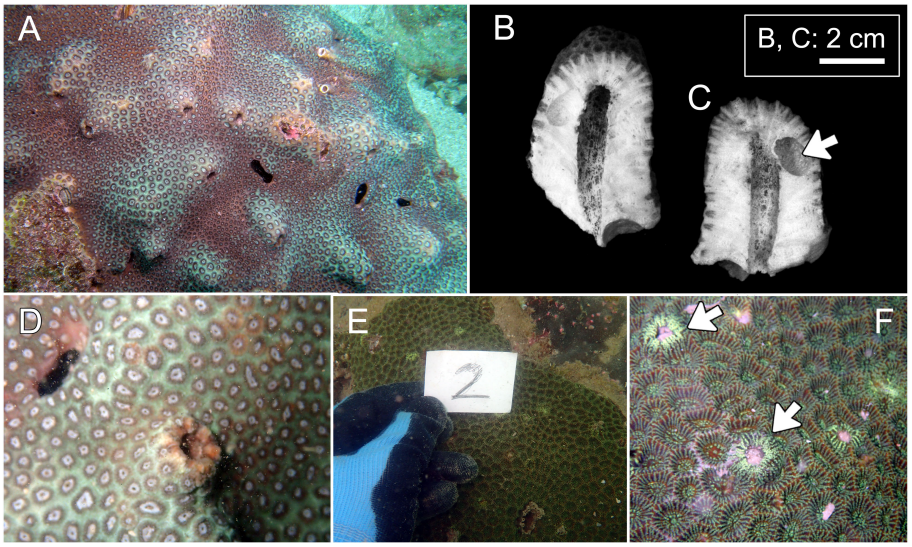

FIGURE 4
Hosts of *Lithoscaptus doughnut* sp. nov. **(A–D)** and *Xynomaia* species **(E, F)**. **(A)** *Plesiastrea peroni*, Basalt Island; **(B)** *Plesiastrea peroni*, Long Ke Tsai. **(E, F)** *Coelastrea aspera*, Pak Lap Tsai. Cross section of domicile of *L. doughnut* sp. nov. **(B, C)** with arrow showing domicile of *Lithophaga* sp. The "2" shown in **(E)** refers to number of field image. Arrow on **(F)** showing domicile openings of *Xyomaia* species.

The sequences were aligned with MUSCLE implemented in MEGA XI (Ver. 11.0.13; https://www.megasoftware.net/; Tamura et al., 2021), and species identification and delimitation by molecular evidence are addressed by phylogenetic affinities and genetic distances. Given close phylogenetic proximity of the Dotillidae and Cryptochiridae under the Thoracotremata (Sun et al., 2022), the sand bubbler crab *Scopimera globosa* (Family Dotillidae) was included as outgroup (accession number LC535358.1). Neighbor-joining (NJ) analysis was performed using Kimura 2-parameter (K2P) distance model, with gaps or missing data treated using "pairwise deletion," and bootstraps values estimated from 1,000 pseudoreplicates implemented were identified for both COI and 16S rDNA markers in MEGA XI.

Levels of K2P genetic distances were also calculated by MEGA XI. Values of genetic distances are indicated as mean ± standard deviation. In terms of genetic distances, interspecific discrepancies published on various thoracotreme crabs are taken into consideration as thresholds for species delimitation. This figure varies from 1.49% between *Parasesarma liho* and *Parasesarma paucitorum* (Shih et al., 2019; both now *Leptarma*), 2.79% between *Paraleptuca crassipes* and *Paraleptuca splendida* (Shih et al., 2012), 4.39% between *Mictyris brevidactylus* and *Mictyris guinotae* (Davie et al., 2010), to 6.25% between *Ocypode stimpsoni* and *Ocypode mortoni* (KJH Wong et al., 2012). These values serve as references in considering thresholds in species delimitation.

Results

Species identification by COI and 16S rDNA sequencing

In total, 27 16S rDNA sequences and 38 COI mtDNA sequences were extracted from our specimens, and another 42 16S rDNA and 49 COI mtDNA sequences downloaded from Genbank were respectively added to both alignments as reference sequences. Accession numbers of query and reference sequences are provided in Table 1. Alignments of 615 and 625 bp were constructed for markers 16s rDNA and COI, respectively. NJ trees that resulted from analyses using the two markers are shown as Figure 6A (16S rDNA) and Figure 6B (COI mtDNA). Based on query and reference sequences, intraspecific K2P distances of cryptochirids have a mean of 1.06 ± 0.76% and interspecific (intrageneric) distances at 7.16 ± 3.27%. The distribution of these values is shown in Figure 7. Among *Lithoscaptus* species, including forms listed as tentative genetic identifications (*Lithoscaptus* sp. A, C, D, Z), this value ranges from 2.80% to 14.97% (mean 9.22 ± 2.60%), and among described species, the lowest pairwise distance was observed between *Lithoscaptus tuerkayi* (KU745732.1) and *Lithoscaptus hellerii* (KU041819.1) at 3.57%. We do not calculate the frequencies of pairwise distances in 16S rDNA sequences due to its poor resolution in performed analyses for identification (as in NJ tree in Figure 6A; see below).

For phylogenetic affinities between query and reference sequences, only one sequence (CEL-Hapa-022) clustered with

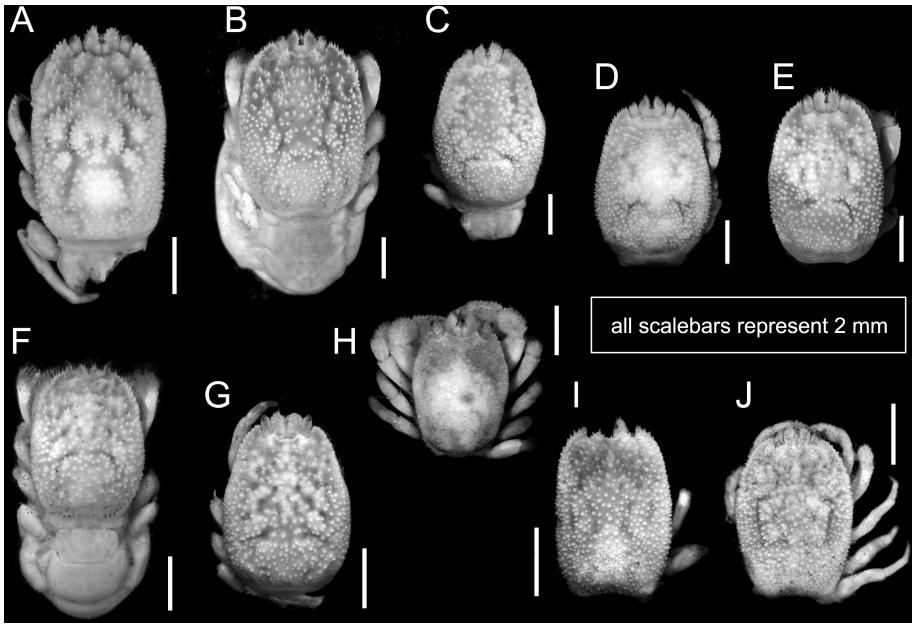

FIGURE 5
Overall habitus of recorded cryptochirids. **(A)** *Cryptochirus coralliodytes* (CEL-Hapa-022); **(B, C)** *Lithoscaptus paradoxus* (CEL-Hapa-013, 007); **(D)** *L. doughnut* sp. nov. (CEL-Hapa-040); **(E)** L. cf. doughnut (CEL-Hapa-006); **(F–J)** *L. scottae* sp. nov. (CEL-Hapa-037, 019, 015); **(I, J)** *Xynomaia species* (CEL-Hapa-002, 004). Carapaces of all specimens denuded. All except **(H)** are female crabs.

available 16S rDNA reference sequence of *C. coralliodytes* collected from New Caledonia (KM114587.1; K2P distance, 0.36%). None of the other 26 sequences clustered with any reference sequences (Figure 6A; Table 2). Analyses on COI sequences provided results of better resolution. Sequences from the local material clustered with four reference sequences with high bootstrap values (>80) and can be differentiated into at least six distinct operative taxonomic units (OTUs). Recognized taxa include *Cryptochirus coralliodytes* (KU041822.1) (CEL-Hapa-022; K2P distance 1.13%) and *Lithoscaptus paradoxus* (KU041825.1, KU041820.1) (CEL-Hapa-007-013, 020, 021, 030, 031, 034, 038, 039, and 041; within-group K2P distance, 1.01 ± 0.64%). Reference sequences KJ923679.1, KJ923680.1, and KU041817.1 were listed as *X. sheni* and KU041835.1 as *Xynomaia* sp. Three of our sequences (CEL-Hapa-004, 005, and 016) sharing the same haplotype with KU041817.1 and KU041835.1 [respectively from Guam (as *X. sheni*; 396 bp) and Indonesia (as *Xynomaia* sp.; 625 bp)]. The shared haplotype of CEL-Hapa-001 and 003 differs from KU041817.1 and KU041835.1 by 5.8% and 4.8% in terms of K2P distance, the discrepancy resulting from missing data of the shorter KU041817 reference sequence. A single individual of CEL-Hapa-002, close to 001 and 003 by K2P distance of 1.62%, differs from KU041817.1 and KU041835.1 by 4.72% and 4.13%, respectively. Among these, six local sequences identifiable as *Xynomaia* species, based on topology of NJ tree (Figure 6B) and genetic distances, at least two distinct OTUs can be recognized. See below for elaborations on the identification of "*X. sheni* species complex."

The remaining 14 COI sequences (CEL-Hapa-015, 017–019, 023–029, and 035–037) form a single clade (within group K2P distance 1.20 ± 0.55%), a sister group to that containing *L. paradoxus*, the latter of which included reference sequences from Guam (KU041820.1) and Indonesia (KU041825.1) (between group K2P distance, 4.05 ± 0.87%). This clade does not cluster or show specific affinities with available reference sequences of *Lithoscaptus*, including four from undescribed species sequenced by van der Meij and Nieman (2016), which were all from northern Sulawesi (for the accession number, see Table 1) and is referred as *L. scottae* sp. nov. Two specimens (CEL-Hapa-006 and 040) retrieved from hosts of the Plesiastreidae, distinct from the rest, differ from each other by a K2P distance of 2.73%, marginal for interspecific divergences. CEL-Hapa-040 is genetically distinct from both *L. paradoxus* and *L. scottae* sp. nov. by 6.00 ± 0.93% and 5.80 ± 0.73%, respectively, whereas CEL-Hapa-006 differs from these two taxa by 3.35 ± 0.73% and 3.31 ± 0.87%. With both only represented by only one specimen each, we tentatively refer the two as *L. doughnut* sp. nov. (CEL-Hapa-040) and *L.* cf. *doughnut* (CEL-Hapa-006). These taxa can be morphologically differentiated by subtle characters and separately addressed under systematic account below, including diagnoses and descriptions of the two new pseudocryptic species of *Lithoscaptus*.

TABLE 1 Source of reference sequences: a, van der Meij, 2014; b, van der Meij, 2015a; c, van der Meij, 2015b; d, van der Meij, 2017; e, van der Meij and Nieman, 2016; f, van der Meij and Reijnen, 2014; g, van der Meij and Schubart, 2014.

Specimen number	Identified species	Site	Collection date	Accession number		Sources	
				16S rDNA	COI	16S rDNA	COI
Query gall crab specimens							
Hapa_001	*Xynomaia sheni* species complex	Long Ke Tsai, Sai Kung	26 November 2019	OP114851	OP103608	This study	
Hapa_002	*Xynomaia sheni* species complex			OP114852	OP103609		
Hapa_003	*Xynomaia sheni* species complex			OP114853	OP103610		
Hapa_004	*Xynomaia sheni* species complex			OP114854	OP103611		
Hapa_005	*Xynomaia sheni* species complex			OP114855	OP103612		
Hapa_006	*Lithoscaptus* cf. *doughnut*			OP114856	OP103613		
Hapa_007	*Lithoscaptus paradoxus*			–	OP103614		
Hapa_008	*Lithoscaptus paradoxus*			–	OP103615		
Hapa_009	*Lithoscaptus paradoxus*	Bluff Island, Sai Kung	26 November 2019	OP114857	OP103616		
Hapa_010_e	*Lithoscaptus paradoxus*	Tai She Wan, Sai Kung	27 November 2019	OP114858	OP103617		
Hapa_011	*Lithoscaptus paradoxus*			OP114859	OP103618		
Hapa_012	*Lithoscaptus paradoxus*			OP114860	OP103619		
Hapa_013	*Lithoscaptus paradoxus*			–	OP103620		
Hapa_014	*Lithoscaptus paradoxus*			OP114861	–		
Hapa_015	*Lithoscaptus scottae* sp. nov.	Pak Lap Tsai, Sai Kung	28 November 2019	OP114862	OP103621		
Hapa_016	*Xynomaia sheni* species complex			OP114863	OP103622		
Hapa_017	*Lithoscaptus scottae* sp. nov.			–	OP103623		
Hapa_018	*Lithoscaptus scottae* sp. nov.			OP114864	OP103624		
Hapa_019	*Lithoscaptus scottae* sp. nov.			OP114865	OP103625		
Hapa_020	*Lithoscaptus paradoxus*	Long Ke Tsai, Sai Kung	28 November 2019	OP114866	OP103626		
Hapa_021	*Lithoscaptus paradoxus*			–	OP103627		
Hapa_022	*Cryptochirus coralliodytes*			OP114867	OP103628		
Hapa_023	*Lithoscaptus scottae* sp. nov.			–	OP103629		
Hapa_024	*Lithoscaptus scottae* sp. nov.			OP114868	OP103630		
Hapa_025	*Lithoscaptus scottae* sp. nov.			OP114869	OP103631		
Hapa_026	*Lithoscaptus scottae* sp. nov.			–	OP103632		
Hapa_027	*Lithoscaptus scottae* sp. nov.			–	OP103633		
Hapa_028	*Lithoscaptus scottae* sp. nov.	Pak Lap Tsai, Sai Kung	28 November 2019	OP114870	OP103634		
Hapa_029	*Lithoscaptus scottae* sp. nov.			OP114871	OP103635		
Hapa_030	*Lithoscaptus paradoxus*			OP114872	OP103636		
Hapa_031	*Lithoscaptus paradoxus*			–	OP103637		
Hapa_033	*Lithoscaptus paradoxus*			–	–		
Hapa_034	*Lithoscaptus paradoxus*			OP114873	OP103638		
Hapa_035	*Lithoscaptus scottae* sp. nov.			OP114874	OP103639		
Hapa_036	*Lithoscaptus scottae* sp. nov.			OP114875	OP103640		
Hapa_037	*Lithoscaptus scottae* sp. nov.			OP114876	OP103641		
Hapa_038	*Lithoscaptus paradoxus*	Bluff Island, Sai Kung	27 November 2019	–	OP103642		
Hapa_039	*Lithoscaptus paradoxus*			OP114877	OP103643		
Hapa_040	*Lithoscaptus doughnut* sp. nov.	Basalt Island, Sai Kung	21 September 2012	–	OP103644		
Hapa_041	*Lithoscaptus paradoxus*	Crescent Island, Mirs Bay	14 November 2018	–	OP103645		

(Continued)

TABLE 1 Continued

Specimen number	Identified species	Site	Collection date	Accession number		Sources	
				16S rDNA	COI	16S rDNA	COI
Reference sequences							
	Cryptochirus coralliodytes			KM114587.1	KU041822.1	*g*	*e*
	Cryptochirus sp.			–	KU041829.1	–	*e*
	Dacryomaia japonica			–	KU041821.1	–	*e*
	Dacryomaia sp.			KM114582.1	KJ923653.1	*g*	*f*
				KJ923714.1	KJ923669.1	*f*	*f*
				KJ923729.1	–	*f*	–
	Dactocarcinus balssi			–	KU041815.1	–	*e*
	Fizesereneia heimi			–	KM491176.1	–	unpublished
				–	KU041831.1	–	*e*
	Fizesereneia latisella			–	KU041832.1	–	*e*
	Fizesereneia panda			–	KM491175.1	–	unpublished
	Fizesereneia sp.			KM114581.1	KJ923651.1	*g*	*f*
				KJ923708.1	–	*f*	–
				KJ923713.1	–	*f*	–
	Fungicola fagei			KJ923706.1	–	*f*	–
				KJ923707.1	–	*f*	–
	Fungicola syzygia			KP192936.1	KP192980.1	*b*	*b*
				KP192937.1	–	*b*	–
				KP192938.1	–	*b*	–
	Fungicola utinomi			KP192935.1	–	*b*	–
				KM114583.1	–	*g*	–
				KP192939.1	KP192979.1	*b*	*b*
	Hapalocarcinus marsupialis			EU743929.1	KX224359.1	unpublished	unpublished
				KJ923716.1	KJ923654.1	*f*	unpublished
				KM114586.1	–	*g*	–
	Hiroia krempfi			–	KU041834.1	–	*e*
	Kroppcarcinus siderastreicola			–	KU041837.1	–	*e*
	Lithoscaptus cf. *helleri*			–	KU041824.1	–	*e*
	Lithoscaptus helleri			–	KU041819.1	–	*e*
	Lithoscaptus paradoxus			–	KU041820.1	–	*e*
				–	KU041825.1	–	*e*
	Lithoscaptus prionotus			KJ923725.1	KJ923664.1	*f*	*f*
				KJ923726.1	KJ923665.1	*f*	*f*
	Lithoscaptus semperi			–	KP688583.1	–	*c*
	Lithoscaptus tri			KJ923732.1	KJ923672.1	*f*	*f*
				KJ923733.1	KJ923673.1	*f*	*f*
				KM114584.1	–	*g*	–
	Lithoscaptus sp. A			–	KU041828.1	–	*e*
	Lithoscaptus sp. C			–	KU041827.1	–	*e*
	Lithoscaptus sp. D			–	KU041823.1	–	*e*
	Lithoscaptus sp. Z			–	KU041830	–	*e*
	Lithoscaptus tuerkayi			–	KU745732.1	–	*d*
	Neotroglocarcinus dawydoffi			KJ923711.1	KJ923649.1	*f*	*f*
				KJ923738.1	–	*f*	–
	Neotroglocarcinus hongkongensis			KJ923718.1	KJ923656.1	*f*	*f*

(Continued)

TABLE 1 Continued

Specimen number	Identified species	Site	Collection date	Accession number		Sources	
				16S rDNA	COI	16S rDNA	COI
				KJ923719.1	–	*f*	–
	Opecarcinus cathyae			–	KM396420.1	–	*a*
	Opecarcinus crescentus			–	MW278312.1	–	unpublished
	Opecarcinus hypostegus			–	KU041838.1	–	*e*
	Opecarcinus lobifrons			KJ923727.1	KJ923666.1	*f*	*f*
				KJ923730.1	–	*f*	–
	Opecarcinus pholeter			–	KU041833.1	–	*e*
	Opecarcinus sierra			–	MW278621.1	–	unpublished
	Pelycomaia minuta			–	KU041826.1	–	*e*
	Pseudocryptochirus viridis			KJ923709.1	KJ923650.1	*f*	*f*
				KJ923710.1	–	*f*	–
				KJ923712.1	–	*f*	–
	Pseudohapalocarcinus ransoni			KJ923728.1	KJ923667.1	*f*	*f*
				KJ923753.1	–	*f*	*f*
	Sphenomaia pyriformis			KJ923752.1	KJ923693.1	*f*	*f*
				KJ923755.1	–	*f*	–
	Troglocarcinus corallicola			–	KU041836.1	–	*e*
	Utinomiella dimorpha			KJ923731.1	KJ923671.1	*f*	*f*
				KM114585.1	–	*g*	–
				KJ923734.1	–	*f*	–
				KX224398.1	–	unpublished	–
	Xynomaia sheni			KJ923739.1	KJ923679.1	*f*	*f*
				KJ923740.1	KJ923680.1	*f*	*f*
				–	KU041817.1	–	*e*
	Xynomaia sp.			–	KU041835.1	–	*e*
	Scopimera globosa	(OUTGROUP)		LC535358.1		Kobayashi et al., 2021	

Systematic account

Superfamily Cryptochiroidea Paul'son, 1875

Family Cryptochiridae Paul'son, 1875

Cryptochirus coralliodytes Heller, 1860

(Figures 5A, 8, 15A)

Cryptochirus coralliodytes Heller, 1860: 370, pl. 4(33–39); Heller, 1861: 19.

? *Lithoscaptus paradoxus*—Paul'son, 1875: 77.

Cryptochirus rugosus Edmondson, 1933: 6, fig. 1, pl. 1.

Troglocarcinus (*Favicola*) *rugosus*—Fize and Serène, 1957: 85, figs. 21, 22, 23A, 25A, 27A–C, pls. 5(7), 6(1–3), 10(D, E).

Favicola rugosa—Takeda and Tamura, 1981a: 43, text-fig. 1, pl. 1.

Cryptochirus coralliodytes—Kropp, 1988a: 873, figs. 1–3; Kropp, 1990: 420, fig. 1 —Wei et al., 2006: 1066, fig. 2A.—Castro, 2011: 111.—van der Meij and Nieman, 2016: app. 1.

Material examined. 1♀ (5.3 × 7.5 mm; CEL-Hapa-022), Long Ke Tsai, Sai Kung, 7 m, 28 Nov 2019, on *Platygyra acuta*.

Diagnosis. Carapace longitudinally ovate, regions well-defined by deep grooves; anteriorly half markedly deflexed, scattered with small acute spines, posterior half lined with clustered rounded tubercules, metagastric region as a dense circular tubercular cluster. Epistome bearing three well-defined longitudinal crest. Female thoracic sternum relative narrow, medially depressed; anterior plate rhomboid, approximately as broad as long, weakly granular; sutures 4/5, 5/6, 7/8 medially interrupted, suture 6/7 medially confluent, sternite 7 median line well defined; gonopore on sternite 6, obliquely ovate, sheltered laterally by an eave-like structure. Plp2 biramous, Plp3 uniramous.

Description (based on CEL-Hapa-022, female 5.3 × 7.5 mm). Carapace 1.4 times longer than broad, anteriorly ovate in outline, posteriorly subquadrate, overall pronouncedly sculptured (Figure 8A); anterior 2/5 depressed, strongly

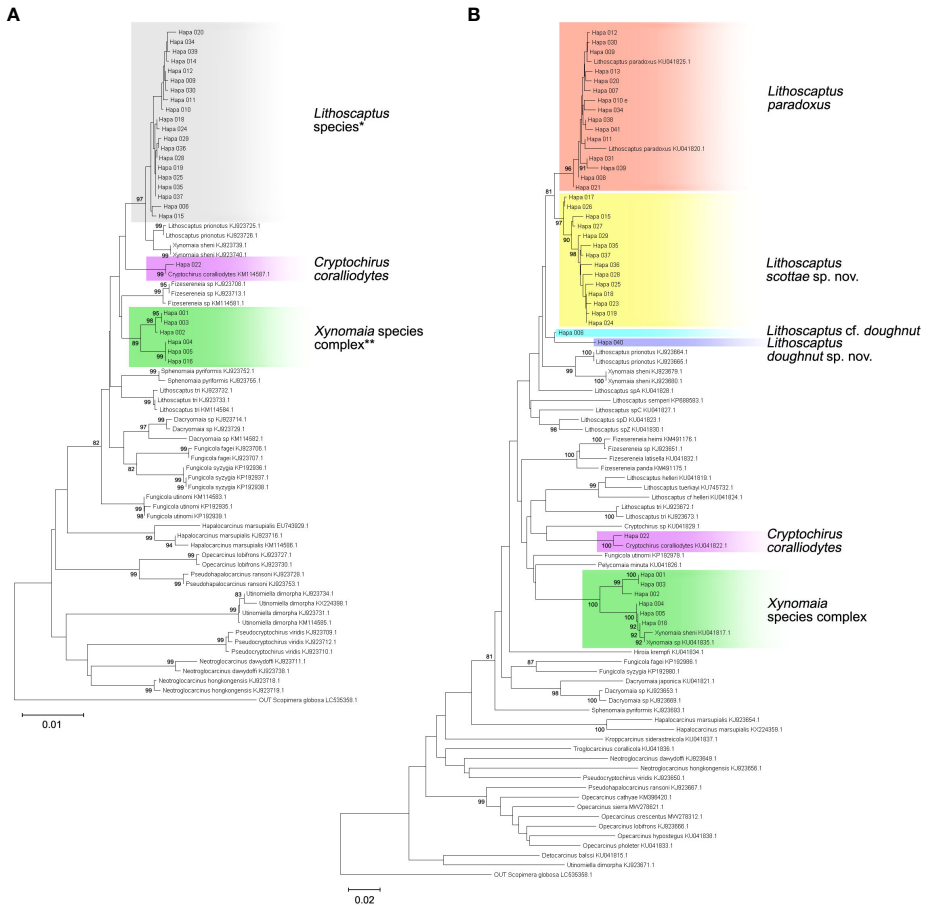

FIGURE 6
Neighbor-joining (NJ) tree of 16S rDNA **(A)** and COI sequences **(B)**. Branch length represents Kimura 2-parameter (K2P) distances, and bootstrap values are shown on the nodes when >80. Details of specimens from the present study (clades highlighted in gray), and reference sequences acquired from Genbank are listed in Appendix 1. Resolution of molecular analyses based on 16S rDNA sequences **(A)** do not allow identification of clades containing *Lithoscaptus* (*) and *Xynomaia* species complex (**). Depictions of both clades are inferred from reconstruction based on COI sequences **(B)**.

deflexed, broadest, and most elevated at approximately half of CL (Figure 8B); front broadly concave, inner orbital lobe convex, inflated, armed with numerous slender spines; mesogastric region scattered with small conical spines, each well-spaced from one another, followed by metagastric region as a circular cluster of densely aligned rounded tubercles, posteriorly separated from cardiac–intestine region by shallow but distinct transverse groove, posterior of which covered with numerous isolated, rounded tubercles; exorbital angle crested, confluent with anterolateral margin, which raised, mildly cristate, lined with series of acute spines, extending to 1/3 of CL; hepatic region depressed, regions at near base of eyestalk and behind inner orbital lobe sunken, giving an eroded texture; proto- and mesobranchial regions lined with three sets of short, deeply incised, oblique grooves, between which each furnished with dense cluster of rounded tubercles: first set lateral to mesogastric region, second lateral to metagastric region, third anterolaterally delineating cardiac–intestine region (Figure 8A). Pterygostomial region mildly granular, completely fused dorsally with carapace (Figure 8B).

Basal plate of antennular peduncle longitudinally ovate, anteriorly armed with series of stout teeth, dorsally depressed, sunken medially, slightly inflated rim lined with flattened granules, ventrally densely granular, nearly flat (Figures 8A, B). Eyestalk short and stout, cylindrical, slightly concave along mesial margin, basal of cornea lined with several small spines on dorsal surface (Figure 8A). Epistome medially elevated, faintly crested, extending to anterior apex along midline, laterally each of a well-defined longitudinal crest (Figure 8C). Mxp3 ischium depressed, covered with low rounded granules, merus distal–external lobe triangular, moderately produced; carpus dilated along internal margin; exopod elongated ovate (Figure 8D). Mxp1 endopod elongated-triangular, mesial margin strongly convex (Figure 8F).

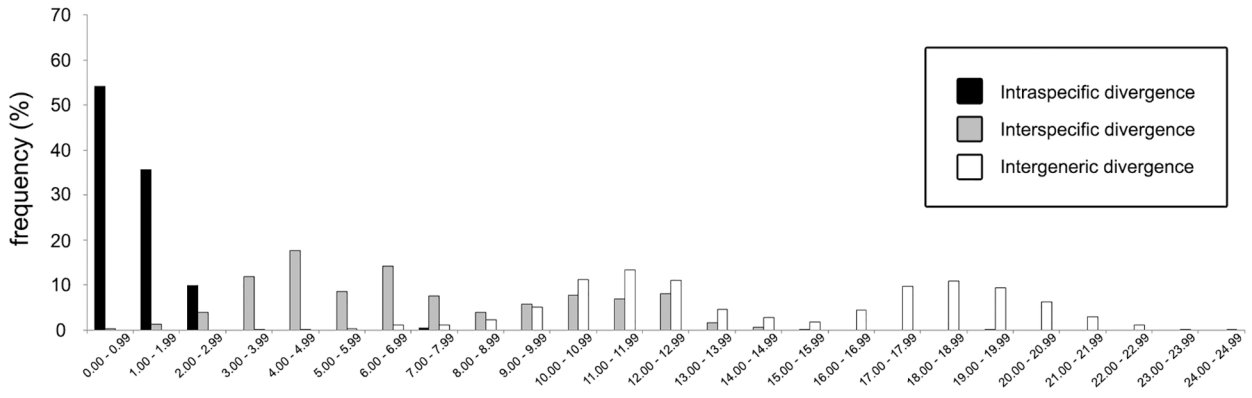

FIGURE 7
Frequency distributions of genetic (K2P) distances based on 87 COI sequences (query and reference) of cryptochirid crabs examined in this study.

Chelipeds symmetrical, much reduced in size, merus to chela compressed; carpus and palm dorsally of small but distinct conical spines; palm externally smooth, fingers slender, shorter than palm, tapering into fine chitinous tips (Figure 8I). P2–P4 short and stout, each merus to propodus externally armed, dactylus shorter than respective propodus, armed with small spinules along extensor margins (Figures 8J–L). P2 merus elongated ovate, 1.9 times longer than broad, distally of several acute spines; carpus and propodus short, subequal in length, externally of series of robust spines (Figure 8J). P3 merus ovate, 1.4 times longer than broad, distally of numerous elongated nodules; carpus and propodus externally of robust spines (Figure 8K). P4 merus ovate, 1.4 times longer than broad, distally of numerous stout nodules; carpus and propodus of numerus rounded nodules (Figure 8L). P5 segments cylindrical, unarmed, surfaces nearly smooth; merus 1.5 times as long as broad; carpus and propodus elongated, subequal in length (Figure 8M); dactylus slender and elongated, curving and articulating ventrally (Figure 8N).

Thoracic sternite anteriorly extending between bases of both Mxp3; anterior plate rhomboid, approximately as long as broad, anteriorly rimmed, medially depressed, surface granular; constriction narrow, less than 1/2 of width of anterior plate, much depressed, grooved along mid-line, confluent with depression along midline; sternites 5 and 6 medially not separated, much depressed along midline; gonopore on sternite 6 as a fine slit, oriented obliquely, opening much sheltered from ventral view by a narrow lateral eave-like extension; suture 6/7 medially nearly confluent, separated medially; sternite 7 median line well defined; suture 7/8 medially separated (Figure 8H). Plp1 and Plp2 biramous, Plp3 uniramous.

TABLE 2 Query and reference sequences examined in the present study.

	No. of new sequences extracted		Intraspecific genetic (K2P) distances		Interspecific genetic (K2P) distances (COI: lower left; 16S: upper right)				
	16S	COI	16S	COI	*C. coralliodytes*	*L. paradoxus*	*L. doughnut* sp. nov.	*L. scottae* sp. nov.	*X. sheni* spp. Complex
Cryptochirus coralliodytes	2	2	0.36%	1.13%	–	4.41 ± 0.41%*	#	4.48 ± 0.33%*	5.27 ± 0.33%*
Lithoscaptus paradoxus	9*	17	0.50 ± 0.21%*	1.01 ± 0.64%	11.31 ± 0.08%	–	#	1.14 ± 0.32%*	5.22 ± 0.23%*
Lithoscaptus doughnut sp. nov.	0#	1	–	–	10.40%	5.99 ± 0.93%	–	#	#
Lithoscaptus scottae sp. nov.	10*	14	0.30 ± 0.26%*	1.20 ± 0.55%	10.48 ± 0.04%	4.05 ± 0.87%	5.80 ± 0.07%	–	2.83 ± 2.31%*
Xynomaia sheni species complex	6*	10	1.60 ± 1.30%*	6.31 ± 5.44%	12.29 ± 0.06%	11.14 ± 2.22%	10.62 ± 1.91%	10.38 ± 2.21%	–

Number of 16S rDNA and COI sequences extracted in this study (left); intraspecific (middle) and matrix of pairwise (right) K2P distances of query and reference sequences. Values are indicated as mean ± standard deviation. Given the poor identification resolution from analyses based on 16S rDNA marker, inferred intra- and interspecific placement is based on that derived from COI sequences (marked with *). No 16S rDNA sequence is extracted from the holotype of *L. doughnut* sp. nov. (#).

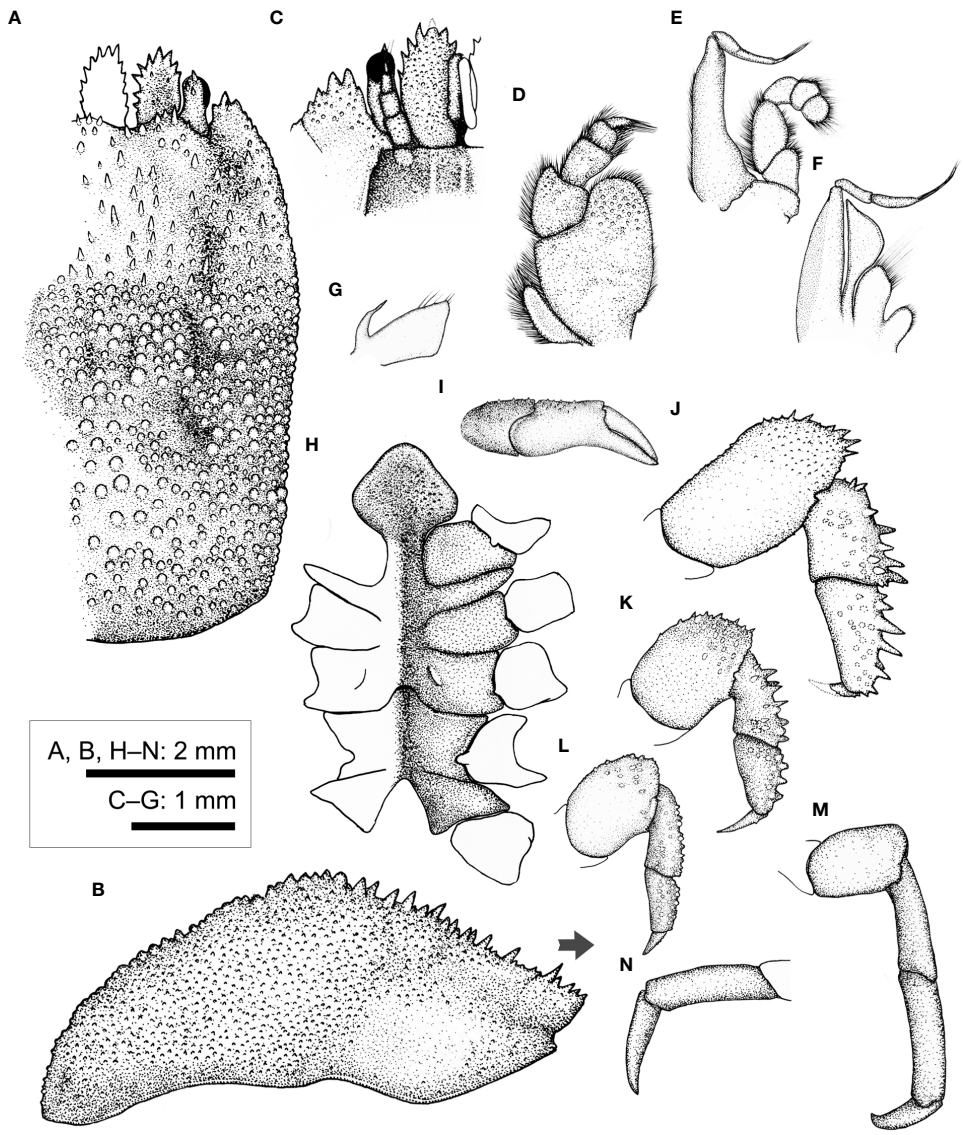

FIGURE 8
Cryptochirus coralliodytes Heller, 1860 (CEL-Hapa-022). **(A)** carapace, dorsal view; **(B)** carapace, lateral view; **(C)** anterior view of carapace, ventral view; **(D)** right Mxp3; **(E)** right Mxp2; **(F)** right Mxp1; **(G)** right Mxl 1; **(H)** thoracic sternites; **(I)** right P1; **(J–M)** right P2 to P5, dorsal view; **(N)** right P5, propodus and dactylus, lateral view. Arrow in **(B)** indicates the anterior direction.

Host coral. Our only specimen, an ovigerous female, had been collected from *P. acuta*. This individual shared the same host community with at two other individuals of *L. paradoxus* (including CEL-Hapa-020). This host species is one of the dominant species in eastern and northeastern waters of Hong Kong (Chan et al., 2005). This species displays a broader range of host preference, which largely of the Merulinidae, and those previously recorded as under the "Faviidae" (note current taxonomic revision of corals indicates Faviidae is restricted to Atlantic, while those Pacific faviid species were transferred to the family Merulinidae; Budd et al., 2012). These include the following: *Coelastrea* (Hiro, 1937), *Dipsastraea* (Edmondson, 1925; Hiro, 1937), *Goniastrea* (Semper, 1881; Hiro, 1937; Fize and Serène, 1957; Wei et al., 2006), *Hydnophora* (Potts, 1915), *Leptoria* (Borradaile, 1902; Potts, 1915), *Merulina* (Takeda and Tamura, 1980), *Paragoniastrea* (Wei et al., 2006), *Platygyra* (Hiro, 1937; Fize and Serène, 1957; Kropp, 1988a; van der Meij and Nieman, 2016), and *Trachyphyllia* (Semper, 1881). Hosts also include various other taxa under the Merulinidae, previously referred to as "Faviidae" and "*Favia*" (for revision of faviid taxa, see Budd et al., 2012) (Edmondson, 1925; Edmondson, 1933; Hiro, 1937; Takeda and Tamura, 1983;

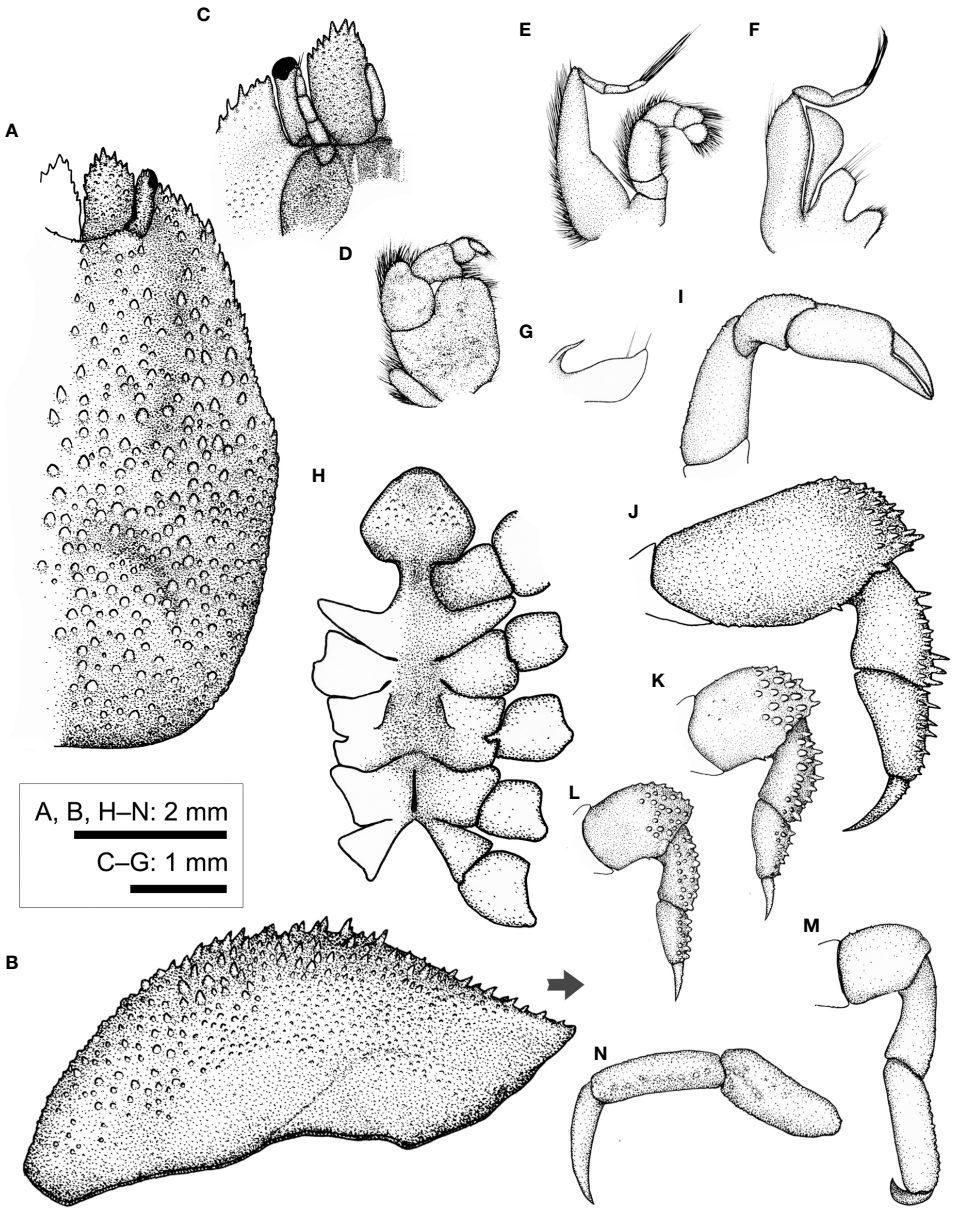

FIGURE 9
Lithoscaptus paradoxus A. Milne-Edwards, 1862, female (CEL-Hapa-007). **(A)** carapace, dorsal view; **(B)** carapace, lateral view; **(C)** anterior view of carapace, ventral view; **(D)** right Mxp3; **(E)** right Mxp2; **(F)** right Mxp1; **(G)** right Mxl 1; **(H)** thoracic sternites; **(I)** right P1; **(J–M)** right P2 to P5, dorsal view; **(N)** right P5, propodus and dactylus, lateral view. Arrow in **(B)** indicates the anterior direction.

Takeda and Tamura, 1985; Davie, 2002; Castro, 2011). Based on material from Port Sudan, Red Sea, Potts (1915) also reported *Leptastrea bottae* (as *L. solida*) of the Leptastreidae.

Type locality. Red Sea.

Geographical distribution. Widespread in the Indo-Pacific: Mauritius (Richters, 1880), Red Sea (Heller, 1860; Heller, 1861; Paul'son, 1875; Kropp, 1988a), Minikoi (Borradaile, 1902), Phuket, Thailand (Ng and Davie, 2002), Nhatrang, Vietnam (Fize and Serène, 1957), Hong Kong, South China (this report), Philippines (Semper, 1881), Lanyu, Taiwan (Wei et al., 2006), Ryukyus and Japanese Archipelago (Takeda and Tamura, 1981a; Takeda and Tamura, 1983; Takeda and Tamura, 1985), Borneo, Malaysia (van der Meij and Nieman, 2016), Australia (McNeill, 1968; Davie, 2002), West and Central Pacific Islands (Hiro, 1937; Kropp, 1988a; Poupin, 1996; Paulay et al., 2003; Poupin, 2005; Richer de Forges and Ng, 2006) and Hawaii (Edmondson, 1925; Edmondson, 1933; Castro, 2011).

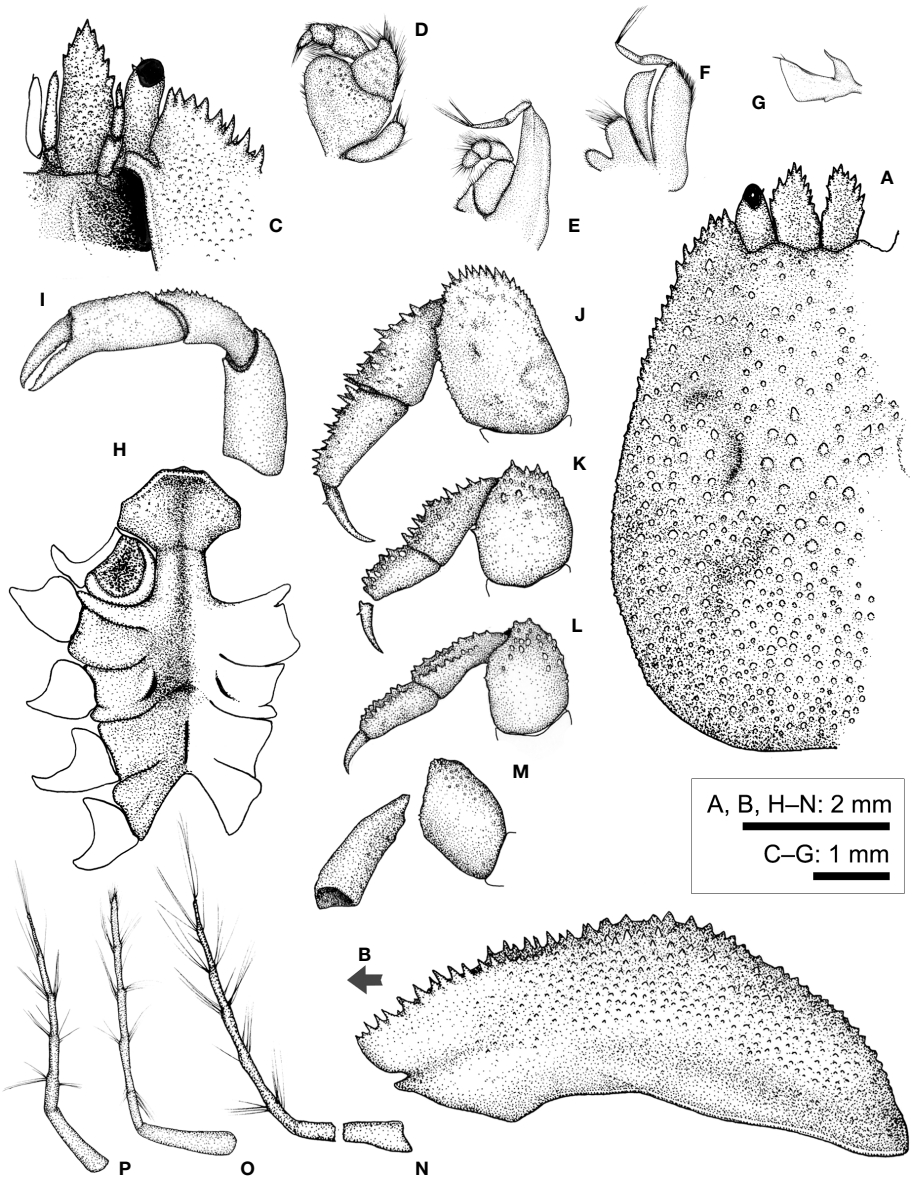

FIGURE 10
Lithoscaptus doughnut sp. nov., female (CEL-Hapa-040). **(A)** carapace, dorsal view; **(B)** carapace, lateral view; **(C)** anterior view of carapace, ventral view; **(D)** left Mxp3; **(E)** left Mxp2; **(F)** left Mxp1; **(G)** left Mxl 1; **(H)** thoracic sternites; **(I)** left P1; **(J–M)** left P2 to P5, dorsal view; **(N–P)** plp1 to plp3, lateral view. Arrow in **(B)** indicates the anterior direction.

Remarks. Taxonomic authority of this species follows the report on decapods described by C. Heller recently compiled by De Grave et al. (2022).

As noted above, the only specimen that we examined (CEL-Hapa-022) was identified as the present species by both genetic markers, which matched the *Cryptochirus coralliodytes* from Malaysia or Indonesia (16S rDNA: KM114587.1) and New Caledonia (COI: KU041822.1) with K2P distance between both, respectively, at 0.36% for and 1.13% (Figures 6A, B; Table 2). For the NJ tree that resulted from analyses on the COI sequences, the clade containing sequences of *C. coralliodytes* from Hong Kong and New Caledonia, despite low support values, shows affiliation, or nested within a lineage inclusive of *Lithoscaptus*, *Xynomaia*, *Fungicola*, and *Pelycomaia* (Figure 6B). *Lithoscaptus* has been demonstrated to be composite by van der Meij and Nieman (2016) (see below). Genetic (K2P) distance at 1.13% for COI falls within the range of intraspecific divergence among cryptochirids (Figure 7).

This species can be morphologically identified from the sympatric *Lithoscaptus* spp. by dorsal ornamentations of

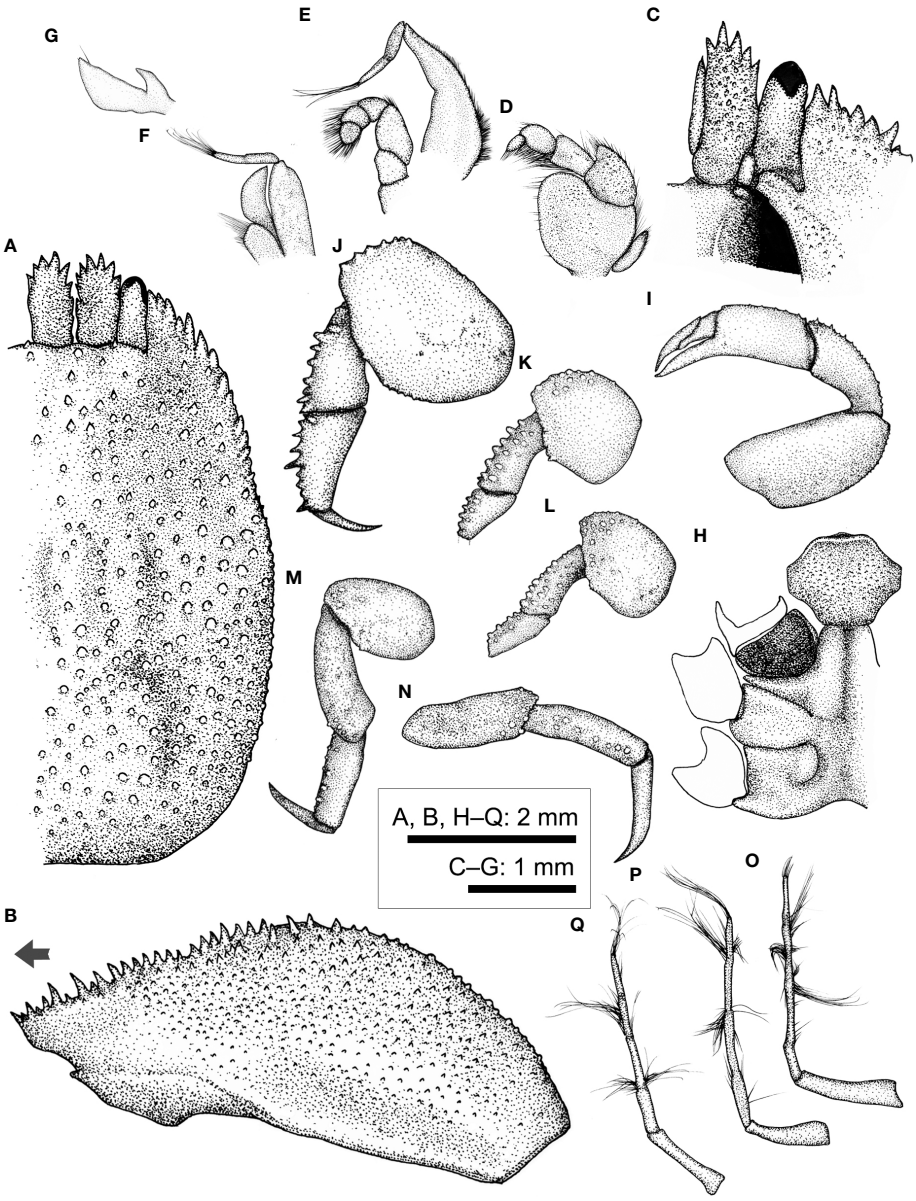

FIGURE 11
Lithoscaptus cf. *doughnut*, female (CEL-Hapa-006). **(A)** carapace, dorsal view; **(B)** carapace, lateral view; **(C)** anterior view of carapace, ventral view; **(D)** left Mxp3; **(E)** left Mxp2; **(F)** left Mxp1; **(G)** left Mxl 1; **(H)** thoracic sternites; **(I)** left P1; **(J–M)** left P2 to P5, dorsal view; **(N)** left P5, lateral view; **(O–Q)** plp1 to plp3, lateral view. Arrow in **(B)** indicates the anterior direction.

carapace, characterized by having more pronounced grooves, and gastric region furnished with dense clump of rounded tubercles (Kropp, 1988a). In this treatment, *Cryptochirus rugosus* Edmondson, 1933 was placed under synonymy of *C. coralliodytes*. As enumerated above, the host range of this species appears to be much broader than other Indo-West Pacific taxa. Past host records would require verification. See Remarks under *L. paradoxus* below.

Lithoscaptus paradoxus A. Milne-Edwards, 1862

(Figures 2, 5B, C, 9, 15B)

Lithoscaptus paradoxus A. Milne-Edwards, 1862: F10.

Cryptochirus coralliodytes var. *fusca* Fize and Serène, 1957: 40, fig. 5B.

Cryptochirus coralliodytes var. *parvula* Fize and Serène, 1957: 40, fig. 5C.

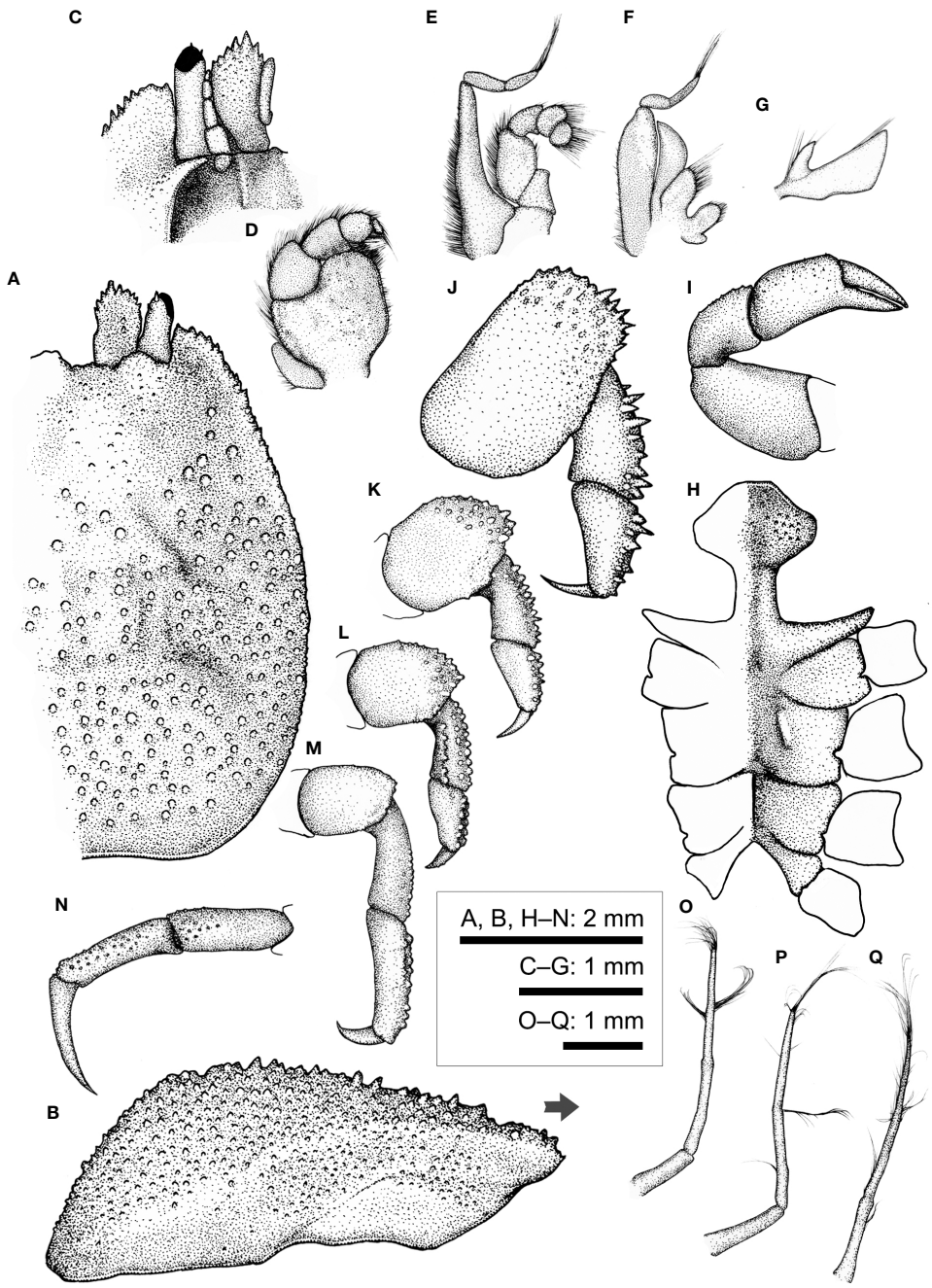

FIGURE 12
Lithoscaptus scottae sp. nov., female (CEL-Hapa-019). **(A)** carapace, dorsal view; **(B)** carapace, lateral view; **(C)** anterior view of carapace, ventral view; **(D)** right Mxp3; **(E)** right Mxp2; **(F)** right Mxp1; **(G)** right Mxl 1; **(H)** thoracic sternites; **(I)** right P1; **(J–M)** right P2 to P5, dorsal view; **(N)** right P5, propodus and dactylus, lateral view; **(O–Q)** Plp1 to Plp3. Arrow in **(B)** indicates the anterior direction.

Cryptochirus coralliodytes var. *rubrolineata* Fize and Serène, 1957: 40, fig. 5D, pl. 14E–H.

Cryptochirus bani Fize and Serène, 1957: 44, figs. 5F, 6, pl. 1(C7).

Lithoscaptus paradoxus—Kropp, 1988a: 877, figs. 4–6 Kropp, 1990: 431, fig. 7.—Paulay et al., 2003: app.—Poupin, 2005: 26.—Richer de Forges and Ng, 2006: 279.—Wei et al., 2006: 1068, fig. 2B.—van der Meij and Nieman, 2016: app. 1.

Material examined. 2♀♀ (5.5 × 7.4 mm, 5.3 × 7.6 mm; CEL-Hapa-007, 008), Long Ke Tsai, Sai Kung, 7–11 m, 26 November 2019, on *Platygyra contorta*; 1♀ (3.9 × 5.7 mm; CEL-Hapa-009), Bluff Island, Sai Kung, 7 m, 27 November 2019; 3♀♀ (5.8 ×

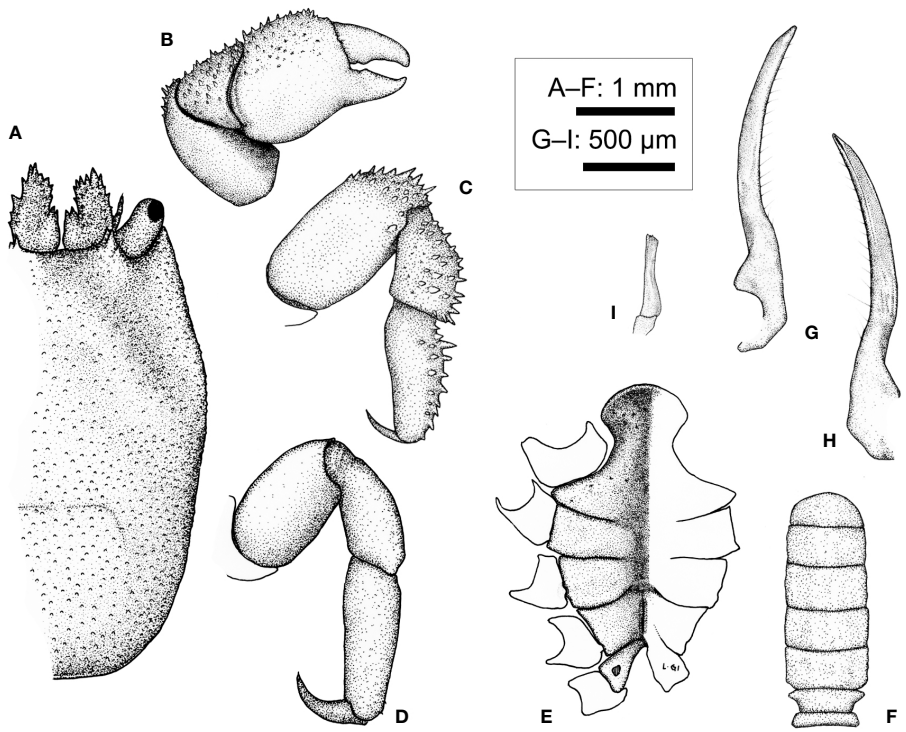

FIGURE 13
Lithposcaptus scottae sp. nov., male (CEL-Hapa-019). **(A)** carapace; **(B)** 1681 right P1; **(C, D)** right P2, P5, dorsal view; **(E)** thoracic sternites, left sternite 8 obscured base of left G1; **(F)** pleon; **(G)** right G1, dorsal view; **(H)** right G1, ventral view; **(I)** right G2, lateral view.

3.1 mm, cw 6.0 mm–5.4 × 7.5 mm; CEL-Hapa-010–012), Tai She Wan, Sai Kung, 27 November 2019, on *P. acuta*; 2♀♀ (5.6 × 7.4 mm, 6.1 × 8.5 mm; CEL-Hapa-013, 014), Tai She Wan, Sai Kung, 27 November 2019, on *P. acuta*; 2♀♀ (4.9 × 7.1 mm, 5.6 × 8.0 mm; CEL-Hapa-020, 021), Long Ke Tsai, Sai Kung, 7 m, 28 November 2019, on *P. acuta*; 4♀♀ (5.7 × 7.8 mm–6.1 × 8.1 mm; CEL-Hapa-030, 031, 033, 034), Pak Lap Tsai, Sai Kung, 28 November 2019, on *P. acuta*; 2♀♀ (4.7 × 6.6 mm, 6.5 × 8.6 mm; CEL-Hapa-038, 039), Bluff Island, Sai Kung, 27 November 2019, on *P. acuta*; 1♀ (4.5 × 6.6 mm; CEL-Hapa-041), Crescent Island, Mirs Bay, 14 November 2018.

Diagnosis. Carapace longitudinally ovate, anterior half depressed, deflexed, regions moderately defined, anteriorly by depression lateral to gastric region, scattered with small conical spines, posterior half of low, well-separated rounded tubercles, cardiac region anteriorly and laterally defined by two arc-shaped grooves, mesially notyt connected. Epistome medially elevated but nor crested, laterally each of one longitudinal crest. Female thoracic sternum relatively narrow, medially depressed, anterior plate spade shaped, approximately as long as broad, surface mildly granular; sutures 4/5, 5/6, and 7/8 medially interrupted, suture 6/7 nearly confluent, sternite 7 medially of well-defined median line; gonopore on sterniten 6 as a narrow, oblique slit, sheltered by a narrow eave-like structure. Plp2 and Plp3 uniramous.

Description (based on CEL-Hapa-007, female 5.5 × 7.4 mm). Carapace longitudinally ovate, 1.3 times as long as broad, broadest, and most elevated at approximately half-CL (Figures 9A, B); anterior half-depressed, markedly deflexed, moderately sculptured, hepatic region lateral to mesogastric region sunken each as an oblique, shallow, broad groove, mesogastric region elevated, scattered with several small acute conical spines, posteriorly defined by two broad clusters of tubercles; cardiac–intestine region anterolaterally defined by deeply incised arc-shaped grooves (⌒ and ⌒), mesially not connected; posterior half of carapace inflated, roundish in outline, overall sparsely covered by rounded tubercles of varying sizes, isolated from each other, diminishing posteriorly (Figure 9A). Front broadly concave, inner orbital lobe each followed by raised granular patch, furnished with several acute spinules; exorbital angle projecting beyond frontal lobes, confluent with anterolateral margin, compressed, margin crested, armed with series of acute spines, extending approximately 1/3 carapace length. Pterygostomial region finely granular, rhomboid plate of which fused dorsally with carapace, suture inconspicuous but discernable (Figure 9A).

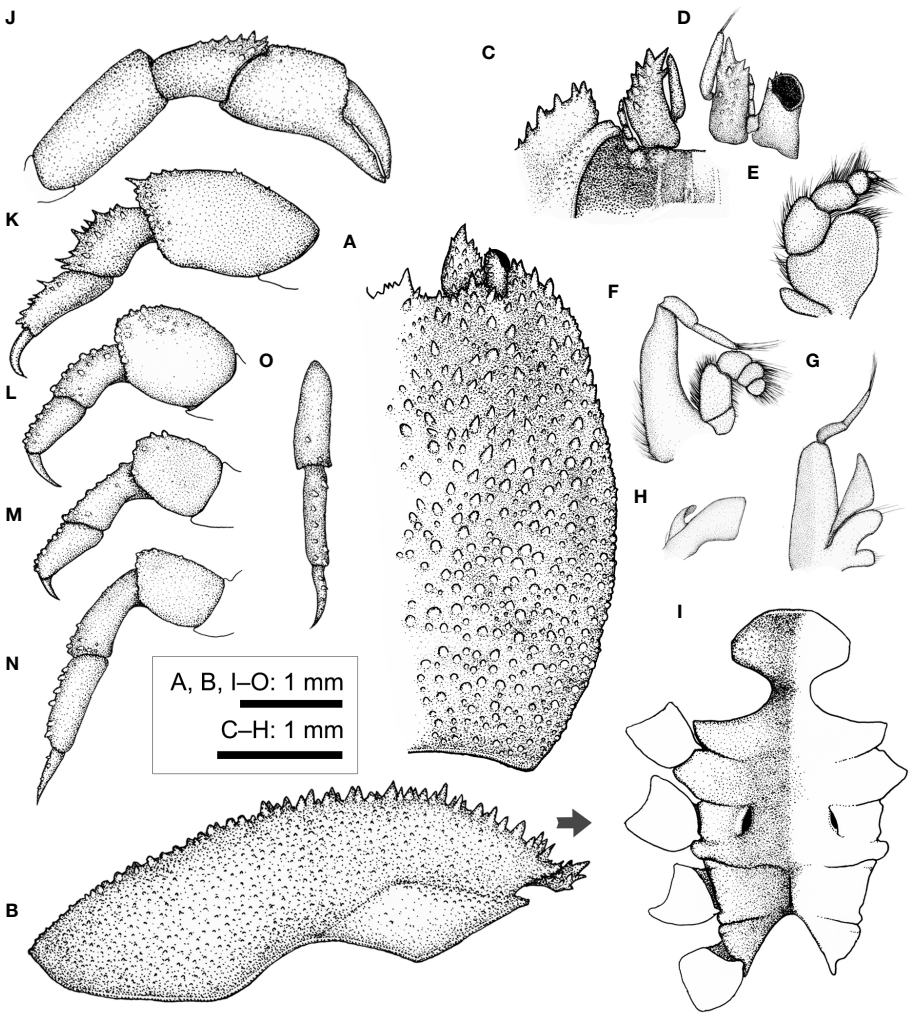

FIGURE 14
Xynomaia sheni (Fize & Serène, 1956) (CEL-Hapa-002). **(A)** carapace, dorsal view; **(B)** carapace, lateral view; **(C)** anterior view of carapace, ventral view; **(D)** left eyestalk and antenna 1 and 2; **(E)** right Mxp3; **(F)** right Mxp2; **(G)** right Mxp1; **(H)** right Mxl1; **(I)** thoracic sternites; **(J)** right P1; **(K–N)** left P2 to P5, dorsal view; **(O)** left P5, carpus to dactylus, lateral view. Arrow in **(B)** indicates the anterior direction.

Basal plate of antennular peduncle longitudinally ovate, dorsally depressed, ventrally mildly inflated, granular, anteriorly armed with series of acute teeth, distally extending beyond respective cornea (Figures 9A, C). Eyestalk stout, cylindrical, nearly straight, cornea extending anterolaterally beyond exorbital angle; cornea spheroidal, mildly expanded, basal of which scatted with several acute spinules on dorsal surface (Figure 9A). Epistome medially elevated, laterally each lined with one longitudinal crest (Figure 9C). Mxp3 ischium depressed, surface rugose, overall furnished with low rounded tubercles, along mesial margin nearly straight; merus distal-externally produced as a rounded lobe, carpus mildly dilated; exopod elongated bean shaped (Figure 9D). Mxp1 endopod mesially arched (Figure 9F).

Cheliped symmetrical, merus to chela strongly compressed, carpus and chela dorsally lined with small spines; chela palm longer than fingers, externally smooth, fingers slender, mildly deflexed, tapering into fine tips (Figure 9I). P2–P4 short and robust, meri compressed, carpi and propodi armed with series of spines or stout nodules, dactyli slender, claw-shaped, shorter than respective dactylus (Figures 9J–L). P2 merus subovate, approximately 2.1 times as long as broad, distally of small stout spines, posteriorly armed with one small spine; carpus and propodus of acute spines; dactylus proximally armed with small spinules on extensor margin (Figure 9J). P3 merus approximately 1.4 times as long as broad, distally of numerous stout spines, posteriorly lined with one small spine; carpus and propodus externally lined with series of acute teeth; dactylus

proximally armed with small spinules on extensor margin (Figure 9K). P4 merus approximately 1.4 times as long as broad, distally of patch of stout nodules, posteriorly lined with small acute spinule; carpus and propodus externally lined with stout nodules (Figure 9L). P5 elongated, segments cylindrical, merus 1.3 times as long as broad, nearly smooth, unarmed; carpus and propodus laterally furnished with numerous flattened, round tubercles; dactylus slender and elongated, tapering into an acute tip, curving and articulating ventrally (Figures 9M, N).

Thoracic sternites anteriorly extending between bases of both Mxp3, anterior plate rounded-rhomboid or "spade-shaped," nearly as long as broad, distally rounded, surface scattered with low, inconspicuous granules, constriction depressed, narrow, width approximately half of that of anterior plate, medially grooved; sternites 5 to 6 medially not separated, strongly depressed; gonopore on sternite 6 as an elongated slit, laterally sheltered by a narrow eave-like structure; sternite 7 medially depressed, median line elaborate, anteriorly separated from sternite 6 by a narrow transverse depression; suture 7/8 medially separated (Figure 9H). Plp1 to Plp3 uniramous.

Host coral. Examined local material has been retrieved from scleractinian hosts of *P. acuta* and *P. contorta*, both species not uncommon among coral communities of Hong Kong (Chan et al., 2005). The range of host preferences of *L. paradoxus* consists largely of the Merulinidae, including *Cyphastrea* sp. (Fize and Serène, 1957 [*C. coralliodytes* var. *parvula*]), *Dipsastraea speciosa* (Fize and Serène, 1957 [*C. bani*; as *Favia*]), *Favites abdita* (Fize and Serène, 1957 [*C. coralliodytes* var. *fusca*]), *Goniastrea pectinata* (Fize and Serène, 1957 [*C. coralliodytes* var. *fusca*; as *G. quoyi*]; Kropp, 1988a), *G. retiformis* (Fize and Serène, 1957 [*C. coralliodytes* var. *parvula*]), *Paragoniastrea australensis* (Wei et al., 2006; as *Goniastrea*), *Platygyra daedalea* (Kropp, 1988a), and *P. lamellina* (Fize and Serène, 1957 [*C. coralliodytes* var. *rubrolineata*]; van der Meij and Nieman, 2016).

Type locality. Reunion Island.

Geographical distribution. Across the Indo-Pacific: Reunion Island (A. Milne-Edwards, 1862; Kropp, 1988a), Nhatrang, Vietnam (Fize and Serène, 1957), Hong Kong, South China (present report), Lanyu, Taiwan (Wei et al., 2006), Ternate, Indonesia (van der Meij and Nieman, 2016), and West Pacific Islands towards French Polynesia (Kropp, 1988a; Kropp, 1990; Paulay et al., 2003; Poupin, 2005; Richer de Forges and Ng, 2006).

Remarks. COI sequences of 15 specimens (CEL-Hapa-007–013, 020, 021, 030, 031, 034, 038, 039, 041) clusters with reference sequences of *L. paradoxus* (KU041825.1: Ternate, Indonesia; KU041820.1: Guam; Figure 6B), with a mean within-group K2P distance at 1.01 ± 0.64%, which is acceptable as an intraspecific value (Figure 7; Table 2).

Kropp (1988a) resurrected *L. paradoxus* and placed several *Cryptochirus* species and varieties described by Fize and Serène (1957) from Nhatrang, Vietnam, under the synonymy of *L. paradoxus*. Both redefined genera can be distinguished by whether Plp2 of females being uniramous (*L. paradoxus*) or biramous (*C. coralliodytes*), along with *Lithoscaptus* having a less as sculptured carapace (Figure 9A *vs.* 8A), epistome medially raised but not ridged (Figure 9C *vs.* 8C), and P5 carpus and propodus laterally tubercular (Figure 9N *vs.* 8N). These observations are consistent with the identification of our material. *Lithoscaptus* can be delineated from other genera by carapace anteriorly deflexed, lack of deep, bowl-shaped concavity, pterygostomial region dorsally fused with carapace, P2 merus lacking distal–mesial projection, and surface of anterior extension of female thoracic sternite smooth (Kropp, 1990).

Two characteristics, however, namely, fusion of pterygostomian plate and surface texture of anterior extension of female thoracic sternites, would require elaboration. In *Lithoscaptus*, the structured was defined as "fused to carapace" (Kropp, 1988a; Kropp, 1990). In our material identified as *L. paradoxus*, *L. doughnut* sp. nov., and *L. scottae* sp. nov., however, we find the pterygostomial plate functionally fused with carapace, but an inconspicuous but discernable suture can be observed. This fine suture can be made visible with application of ethanol-soluble dye and indicated in the line drawings herein provided (*L. paradoxus*: Figure 9B; *L. doughnut*: Figure 10B; *L.* cf. *doughnut*: Figure 11B; *L. scottae*: Figure 12B). In contrast, this suture is completely absent in *C. coralliodytes* (Figure 8B) but more visible in our *Xynomaia* species (Figure 14B). In describing *L. prionotus*, a somewhat aberrant member under the genus, Kropp (1994) casted doubt on whether the form of pterygostomial region can be considered one of the diagnostic features of the genus. As for the surface texture of anterior plate of female thoracic sternum, the structure was reported to be furnished with transverse band of granules in *C. coralliodytes* while smooth in *L. paradoxus* (Kropp, 1990). Among our material, that of *C. coralliodytes* is indeed granular (Figure 8H), while those of *L. paradoxus*, *L. doughnut*, *L.* cf. *doughnut*, and *L. scottae* are finely granular and/or punctate (Figures 9H, 10H, 11H, and 12H, respectively). Among past records of this genus, the latter had generally been neglected as a potential diagnostic feature, and the structure was illustrated for only 3 out of 10 previously described species [*L. paradoxus*: fig. 4c in Kropp (1988a); *L. prionotus*: fig. 4c in Kropp (1994); *L. tuerkayi*: fig. 4b in van der Meij (2017)]. With *Lithoscaptus* shown heterogeneous (van der Meij and Nieman, 2016), we herein recommend consideration and include female thoracic sternites as a potential diagnostic morphological feature of *Lithoscaptus* and relevant genera. See further elaborations under *General Discussions* below.

Lithoscaptus doughnut sp. nov.

(Figures 4A–C, 5D, 10)

urn:lsid:zoobank.org:act:069CFE5E-EFFD-4C18-8741-7ECA919FB7C6

Material examined. Holotype ♀ (6.2 × 8.4 mm; CEL-Hapa-040/ASIZCR), Basalt Island, Sai Kung, 21 September 2012, on *Plesiastrea peroni*.

Diagnosis. Carapace longitudinally ovate, broader posteriorly, anterior half depressed, regions mildly defined, surface of scattered, isolated rounded tubercles interspaced with short conical spines, metagastric region laterally each defined by brachet-shaped groove. Epistome of two longitudinal crests. Female thoracic sternum relatively narrow, medially depressed, anterior plate transversely octagonal, 1.6 times broader than long, surface mildly granular, strongly sculptured; sutures 4/5, 5/6, and 7/8 medially interrupted, suture 6/7 nearly confluent; sternite 7 medially of well-defined median line; gonopore on sternite 6 as an oblique slit, laterally sheltered by an eave-like structure. Plp2 and Plp3 uniramous.

Description (based on Holotype CEL-Hapa-040, female 6.2 × 8.4 mm). Carapace longitudinally ovate, 1.4 times as long as broad, broadest, and most elevated at approximately half-CL; anterior half depressed, markedly deflexed, hepatic region sunken, strongly sculptured, posterior half inflated, roundish in outline, overall covered by rounded tubercles, well isolated from each other, diminishing near posterior margin; front feebly convex, inner orbital lobe rounded-triangular, inflated, mildly protruding anteriorly, exorbital angle projecting beyond inner orbital lobes, confluent with anterolateral margin, crested, lined with series of slender, acute teeth, extending about 2/5 of CL; gastric region triangular, mildly inflated, sparsely furnished by small, indistinct tubercles, mesogastric region laterally each defined by a well-incised bracket-shaped longitudinal groove; cardiac–intestine region well-defined antero-laterally by deep, oblique grooves; both not connect medially (Figures 10A, B). Pterygostomian region finely granular, rhomboid plate of which fused dorsally with carapace, suture discernible (Figure 10B).

Basal plate of antennular peduncle elongated, dorsally depressed, ventrally cylindrical, granular, anteriorly armed with series of strong acute teeth, projecting beyond tip of cornea (Figures 10A, C). Eyestalks stout, cylindrical, nearly straight, subdistally armed with small acute spinules below cornea, cornea spheroidal, extending beyond exorbital angle (Figure 10A). Epistome along anterior margin slightly sunken and punctated medially, laterally each lined with one faint longitudinal crest, distally not reaching anterior margin (Figure 10C). Mxp3 ischium depressed, rugose, mesial–distal lobe furnished with small rounded granules; merus distal–external angle produced; carpus mildly dilated; expopod elongated bean-shaped (Figure 10D). Mxp1 endopod mesially arched (Figure 10F).

Cheliped symmetrical, merus to chela compressed; dorsal margins of carpus and palm lined with fine spinules; chela palm longer than fingers, external surface smooth; fingers slender, moderately deflexed, tapering into fine chitinous tips (Figure 10I). P2–P4 short and robust, overall decreasing in size and acuteness of armature, meri of all compressed, each carpi and propodi externally lined with acute spines, dactyli shorter than respective propodus (Figures 10J–M). P2 merus longitudinally ovate, 1.6 times as long as broad, distally armed with series of similar-sized acute teeth, posteriorly lined with inconspicuous granules, dactylus slender, shorter than propodus, externally armed with small spine (Figure 10J). P3 merus 1.2 times as long as broad, distally of small spines and nodules, posteriorly of one stout spine, dactylus externally armed with small spine (Figure 10K). P4 merus 1.4 times as long as broad, posteriorly of one small spine, distally of blunt nodules (Figure 10L). P5 merus robust, nearly cylindrical, anteriorly of small tubercles, carpus elongated, externally of small tubercles (Figure 10M).

Thoracic sternite anteriorly extending between bases of both Mxp3, anterior plate sub-octagonal, 1.6 times broader than long, surface finely granular and strongly sculptured, anteriorly strongly rimmed, depressed along midline; constriction broad, approximately half of anterior plate width, medially interrupted by deep longitudinal groove, depression of which extending to sternite 6; sternites 5 to 6 medially strongly depressed, not separated along midline; gonopore on sternite 6 as an oblique, elongated slit, laterally sheltered by a narrow eave-like structure; suture 6/7 medially confluent; sternite 7 medially depressed, median line elaborate, anteriorly separated from sternite 6 by a shallow, transversely rhomboid depression; suture 7/8 medially separated (Figure 10H). Plp1 to Plp3 uniramous (Figures 10N–P).

Host coral. *Plesiastrea peroni* of the Plesiastreidae.

Etymology. Specific epithet alludes to the loose resemblance between corallites of the host coral with the sugary treat, in the eyes of a snack-indulged graduate student. The name is used here as a noun in apposition.

Type locality. Basalt Island, Sai Kung, Hong Kong.

Geographical distribution. So far only from type locality.

Remarks. The genus *Lithoscaptus* now contains 12 described species (updated from Ng et al., 2008), and recent descriptions include *L. semperi* van der Meij, 2015b, *L. tuerkayi* van der Meij, 2017, and in the present study, *L. doughnut* sp. nov. and *L. scottae* sp. nov. Several Indo-Pacific forms, being genetically distinct, are yet formally described (van der Meij and Nieman, 2016). As demonstrated by van der Meij and Nieman (2016), this genus is clearly heterogeneous, with genera such as *Cryptochirus*, *Pelycomaia*, and *Xynomaia* nested within (see below).

For the host of *L. doughnut* sp. nov., the coral genus *Plesiastrea* currently comprises of two species, including *P. versipora*, which were once considered to be the single species distributing across the Indo-Pacific but now shown to confined to temperate waters of southern Australia and a recently resurrected *P. peroni*, a tropical species (Juszkiewicz et al., 2022). The family Plesiastreidae is now first reported as a host species of cryptochirid crabs. This host species had long been

placed under the Faviidae *sensu lato*, but recent molecular data showed which represents a distinct lineage under the "robust group," basal to multiple genera of the Merulinidae and Montastraeidae (Fukami et al., 2008; Benzoni et al., 2011; Arrigoni et al., 2012). The association is also surprising among *Lithoscaptus* species, which are all largely symbionts of the Merulinidae (sensu Huang et al., 2014).

Apart from an unique host taxa, the morphology of *L. doughnut* sp. nov. falls under definitions of the genus (as indicated under *L. paradoxus* above) in the following aspects: (1) much deflexed anterior portion of carapace, dorsally covered by small isolated, not clustered spines and tubercles; (2) lacking bowl-shaped cavities; and (3) P2 merus lacking distal–mesial extension. *Lithoscaptus doughnut* sp. nov., however, differs from other described congeners in the following aspects: (1) ornamentation and armature of carapace: mesogastric region of *L. doughnut* laterally defined by shallow, broad depression, metagastric region laterally defined by a set of bracket-shaped (] [) deep grooves (Figures 5D, 10A). A number of congeners have laterally grooved metagastric regions but all differ in the following aspects: (1) anterolateral margin of *L. grandis* interrupted, defining one spinose lobe behind exorbital angle [fig. 1A in Takeda and Tamura (1983)]; in *L. helleri* mesogastric region defined by deep, oblique grooves [fig. 24 in Fize and Serène (1957)]; that of *L. paradoxus* of broad, shallow depression [fig. 7a in Kropp (1990); Figures 5D, 9A); of *L. prionotus* both meso- and metagastric regions defined by deep, broad, oblique grooves, the latter confluent with cardiac–intestine grooves [fig. 4a in Kropp (1994)]; and in *L. tuerkayi*, furnished with deep depression posterior to orbits and flanking mesogastric region [figs. 1A, 4A in van der Meij (2017)]; (2) Morphology of female thoracic sternites: anterior plate of *L. doughnut* transversely sub-octagonal, surface strongly sculptured, constriction relatively broad, more than 1/2 width of anterior plate (Figures 10H), in comparison with those congeners being rounded-rhomboid, approximately as long as broad as in *L. paradoxus* [fig. 7c in Kropp (1990)], octagonal and approximately as long as broad in *L. prionotus* [fig. 4c in Kropp (1994)], and transversely ovate as in *L. tuerkayi* [fig. 4B in van der Meij (2017)]. (3) Overall shape of P2 merus of *L. doughnut* being elongated ovate, approximately 1.6 times as long as broad. The relative length of this segment is intermediate among congeners, which range from outline circular, 1.1 times as long as broad in *L. semperi* [fig. 1g van der Meij (2017)], elongated ovate and approximately 1.5 times in *L. paradoxus* [fig. 7d in Kropp (1990)] and *L. prionotus* [fig. 4e in Kropp (1994)], 1.8 times, bearing strong distal spines in *L. tuerkayi* [fig. 2B in van der Meij (2017)] to twice or above in *L. pacificus* [fig. 2f in Edmondson (1933)] and *L. pardalotus* [fig. 4e in Kropp (1995)].

Although the clade containing both specimens from *Plesiastrea* remains poorly supported (Figure 6B) and does not cluster with any reference sequences, genetic distances between *L. doughnut* sp. nov. and other congenerics lend support to the above morphological distinctions. So far, 14 COI sequences from material identified as *Lithoscaptus* species have been deposited in GenBank, representing six described species, including *L. helleri*, *L. paradoxus*, *L. prionotus*, *L. semperi*, *L. tri*, and *L. tuerkayi*, in addition to five undescribed forms, *L.* cf. *helleri*, and spp. A, C, D, and Z (Table 1). Among our local material, *L. doughnut* (n = 1) differs, in terms of K2P genetic distance from *L. paradoxus* (n = 17) by an average of 6.00 ± 0.93%, *L. scottae* sp. nov (n = 14) by 5.80 ± 0.73%, *C. coralliodytes* (n = 2) by 10.40%, and *Xynomaia* species (n = 10) by 10.62 ± 1.91%. Regarding genetically distinct but yet formally described congenerics, *L. doughnut* sp. nov. shows affiliations with, but differs from, *L.* sp. D (KU041823.1) at 6.10%, to 12.96% from *L.* cf. *helleri* (KU041824.1) (Table 3). These values fall within range of interspecific divergences (Figure 7), showing *L. doughnut* sp. nov. being distinct.

For another resembling form found infesting also *P. peroni*, with likewise one female specimen examined, despite considerable morphological distinctions and moderate genetic distance, we prefer to stay conservative in reporting which is *L.* cf. *doughnut* as below, at least for the time being.

Lithoscaptus cf. *doughnut*

(Figures 4D, 5E, 11)

Material examined. ♀ (4.8 × 6.8 mm; CEL-Hapa-006), Long Ke Tsai, Sai Kung, 7–11 m, 26 November 2019, on *P. peroni*.

Description (based on CEL-Hapa-006, female 4.8 × 6.8 mm). Carapace longitudinally ovate, 1.4 times as long as broad, broadest, and most elevated at approximately half-CL (Figures 11A, B); anterior half depressed, markedly deflexed, hepatic region sunken, strongly sculptured, more invaginated lateral to inner orbital lobes; posterior half inflated, roundish in outline, overall covered by rounded, bead-like tubercles of similar sizes, well isolated from each other, diminishing near posterior margin; front nearly transverse, lined with minute spines; inner orbital lobe broad-triangular, inflated, anteriorly armed with small slender spines, exorbital angle projecting, cristate, confluent with anterolateral margin, lined with series of slender, conical teeth, extending about 2/5 of CL; gastric region broad-triangular, mildly inflated, sparsely furnished by small, indistinct tubercles, mesogastric region lined by two broad, short longitudinal groove, laterally each defined by a much deeper, well-incised short longitudinal groove; cardiac–intestine region well defined anterolaterally by deeply incised arc-shaped grooves (⌒ and ⌒), both not connect medially (Figure 11A). Pterygostomian region finely granular, rhomboid plate of which fused dorsally with carapace, suture discernible (Figure 11B).

Basal plate of antennular peduncle elongated, dorsally compressed, ventrally cylindrical, granular, anteriorly armed with series of strong acute teeth, projecting beyond tip of cornea (Figures 11A, C). Eyestalks stout, cylindrical, nearly straight, subdistally armed with small acute spinules below cornea, cornea spheroidal, extending beyond exorbital angle

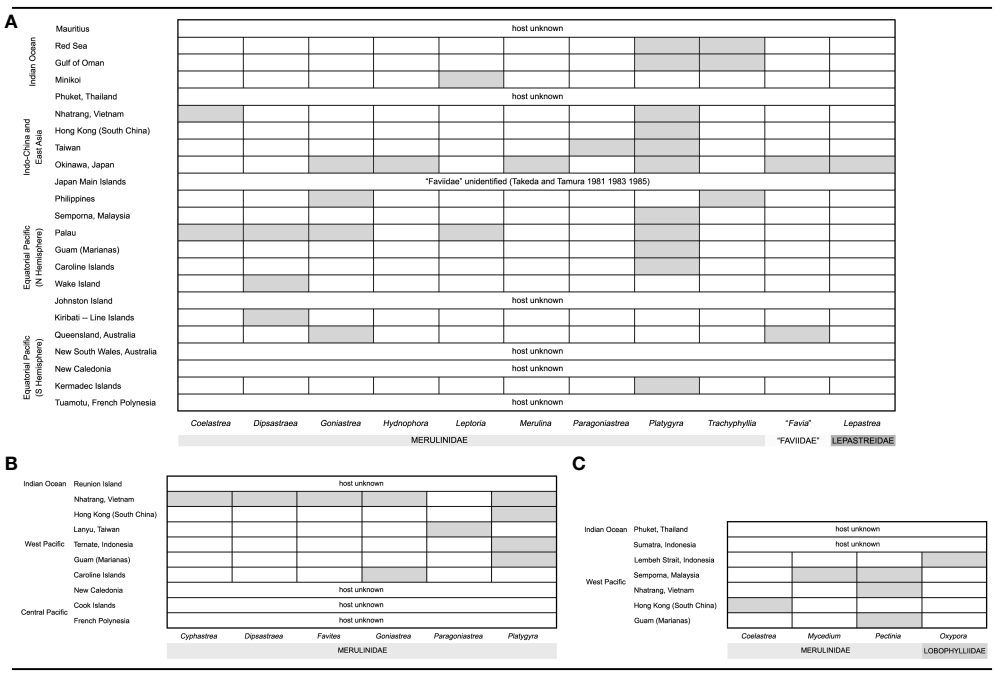

FIGURE 15
Host-distribution figures of three described species of cryptochirid crabs from the literature. The vertical column shows regions of occurrences, and the horizontal row shows hosts of genera reported. Tentative host identifications as familial levels are omitted. **(A)** *Cryptochirus coralliodytes* (Sources: Heller, 1860 1861; Paul'son, 1875; Richters, 1880; Semper, 1881; Borradaile, 1902; Chilton, 1911; Potts, 1915; Edmondson, 1925; Edmondson, 1933; Hiro, 1937; Utinomi, 1944; Fize and Serène, 1957; McNeill, 1968; Takeda and Tamura, 1981a; Takeda and Tamura, 1983; Takeda and Tamura, 1985; Kropp, 1988a; Kropp, 1990; Poupin, 1996; Davie, 2002; Ng and Davie, 2002; Paulay et al., 2003; Poupin, 2005; Richer de Forges and Ng, 2006; Wei et al., 2006; Castro, 2011; van der Meij and Nieman, 2016). **(B)** *Lithoscaptus paradoxus* (Sources: **(A)** Milne-Edwards, 1862; Fize and Serène, 1957; Kropp, 1988a; Kropp, 1990; Paulay et al., 2003; Poupin, 2005; Richer de Forges and Ng, 2006; Wei et al., 2006; van der Meij and Nieman, 2016). **(C)** *Xynomaia sheni*: so far, four distinct COI haplotypes have been recognized, the genetic distance among which suggesting inter-specific divergence (see main text). Three of these haplotypes were found among our six specimens from Hong Kong. Which of these haplotypes represent the "real" *X. sheni* remains unknown. (Sources: Fize and Serène, 1957; Takeda and Tamura, 1981b; Kropp, 1990; Ng and Davie, 2002; Paulay et al., 2003; van der Meij and Reijnen, 2014; van der Meij and Nieman, 2016).

(Figures 11A, C). Epistome medially slightly raised posteriorly, laterally each lined with one distinct longitudinal crest, distally not reaching anterior margin (Figure 11C). Mxp3 ischium depressed, rugose, mesial–distal lobe furnished with low rounded granules; merus distal–external angle weakly produced; carpus mildly dilated; expopod elongated ovate (Figure 11D). Mxp1 endopod mesially arched (Figure 11F).

Cheliped symmetrical, merus to chela compressed; carpus and palm dorsally lined with fine spinules; chela palm longer than fingers, external surface smooth, fingers slender, moderately deflexed, tapering into fine chitinous tips (Figure 11I). P2–P4 short and robust, overall decreasing in size and acuteness of armature, meri of all compressed (Figures 11J–L). P2 merus elongated sub-pentagonal, 1.4 times as long as broad, distally armed with series of blunt conical nodules, similar-sized acute teeth, posteriorly lined with inconspicuous teeth; carpus and propodus externally lined with series of acute spine, dactylus slender, shorter than propodus, externally unarmed (Figure 11J). P3 merus 1.2 times as long as broad, distally of low-rounded tubercles, posteriorly of one blunt tooth, carpus and propodus of series of stout nodules, dactylus externally armed with small spine (Figure 11K). P4 merus 1.4 times as long as broad, distally of low tubercles, posteriorly of inconspicuous tooth, carpus and propodus lined with rounded granules (Figure 11L). P5 robust, segments nearly cylindrical, merus anteriorly of small tubercles, carpus and propodus elongated, subequal in length, externally of small rounded tubercles, dactylus claw-shaped, slender, tapering into a fine tip, curving and articulating ventrally (Figures 11M, N).

Thoracic sternite anteriorly extending between bases of both Mxp3, anterior plate suboctagonal, 1.3 times broader than long, surface coarsely granular, strongly sculptured, anteriorly strongly rimmed, depressed anteriorly; constriction broad, more than half of anterior plate width, strongly inflated as two longitudinally ovate lobes, medially interrupted by deep longitudinal groove, depression of which extending throughout sternite 5; sternites 5 to 6 medially mildly depressed, not separated along midline; gonopore on sternite 6 as an oblique, elongated slit, laterally sheltered by a longitudinally ovate eave-

TABLE 3 Matrix of percentage pairwise nucleotide (K2P) divergence between COI sequences within and between groups of recognized *Lithoscaptus* species.

	No. of sequences (COI)	Interspecific (COI)												
	***L. doughnut* sp. nov.**	***L.* cf. *doughnut***	***L. helleri***	***L.* cf. *helleri***	***L. paradoxus***	***L. prionotus***	***L. scottae* sp. nov.**	***L. semperi***	***L. tri***	***L. tuerkayi***	***L.* sp. A**	***L.* sp. C**	***L.* sp. D**	***L.* sp. Z**
Lithoscaptus doughnut sp. nov.	1	–												
Lithoscaptus cf. *doughnut*	1	2.73%	–											
Lithoscaptus helleri	1	11.48%	10.32%	–										
Lithoscaptus cf. *helleri*	1	12.96%	12.38%	4.08%	–									
Lithoscaptus paradoxus	17	6.00 ± 0.93%	3.35 ± 0.73%	10.34 ± 1.15%	12.37 ± 0.78%	–								
Lithoscaptus prionotus	2	7.15%	4.22%	10.31%	13.94%	6.08 ± 0.61%	–							
Lithoscaptus scottae sp. nov.	14	5.80 ± 0.73%	3.31 ± 0.87%	11.05 ± 0.50%	12.73 ± 0.39%	4.05 ± 0.87%	5.80 ± 0.48%	–						
Lithoscaptus semperi	1	7.50%	6.36%	14.40%	14.94%	9.00 ± 0.74%	9.15%	8.39 ± 0.73%	–					
Lithoscaptus tri	2	10.40 ± 0.27%	9.37 ± 0.45%	10.49 ± 0.42%	11.00 ± 0.27%	11.22 ± 0.90%	9.85 ± 0.44%	10.75 ± 0.58%	11.76 ± 0.28%	–				
Lithoscaptus tuerkayi	1	12.60%	11.97%	3.57%	6.79%	12.15 ± 0.56%	13.55%	12.59 ± 0.44%	14.96%	10.02 ± 0.27%	–			
Lithoscaptus sp. A	1	6.96%	5.19%	12.56%	11.72%	6.48 ± 0.68%	6.96%	6.33 ± 0.59%	9.90%	10.44 ± 0.54%	11.54%	–		
Lithoscaptus sp. C	1	7.13%	5.59%	10.27%	11.37%	7.56 ± 0.69%	8.77%	7.50 ± 0.72%	8.75%	9.33 ± 0.28%	12.00%	8.02%	–	
Lithoscaptus sp. D	1	6.10%	4.06%	7.93%	11.17%	7.21 ± 0.69%	7.52%	6.23 ± 0.71%	8.42%	9.47 ± 0.27%	11.02%	6.07%	6.24%	–
Lithoscaptus sp. Z	1	6.28%	4.25%	7.93%	11.96%	7.44 ± 0.76%	7.70%	6.25 ± 0.82%	8.42%	9.85 ± 0.27%	11.41%	7.16%	5.89%	2.80%	–

Values are indicated as mean ± standard deviation. Examined sequences include query and reference sequences from GenBank (accession no. of which are listed in Table 1).

like structure (Figure 11H). Plp1 to Plp3 uniramous (Figures 11O–Q).

Remarks. Both the present species and *L. doughnut* sp. nov. described above shared host *P. peroni*, a scleractinian coral common in southern and eastern waters of Hong Kong (Chan et al., 2005).

The only acquired female specimen (CEL-Hapa-006) was damaged, with thoracic sternites laterally and posteriorly detached. Various diagnostic morphological features can still be examined and illustrated herein. The present form shares much resemblance with *L. doughnut* sp. nov. but nevertheless identifiable from which and other congeners by the following aspects: (1) metagastric region furnished with two shallow longitudinal grooves, laterally defined by two deeper grooves (Figures 5E, 11A); (2) female thoracic sternum anterior plate octagonal, strongly sculptured, medially markedly grooved along midline (Figure 11H); and (3) P2 merus 1.4 times as long as broad, sub-pentagonal (Figure 11J). See *Remarks* under *L. doughnut* sp. nov. above for distinctions against other congeners.

COI sequence obtained from the only specimen of this form was shorter, with length only 567 bp. Comparing against *L. doughnut* sp. nov. (n = 1) from the same host species, K2P distance was measured to be 2.73%, a value marginal for species recognition (see Figure 7). Surprisingly, among local material examined, *L.* cf. *doughnut* shows affiliation with both *L. paradoxus* (n = 17) and *L. scottae* sp. nov. (n = 14): differing from *L. paradoxus* on average by 3.35 ± 0.73% and *L. scottae* sp. nov. by 3.31 ± 0.87%. As such, genetic distance between *L.* cf. *doughnut* and *L. doughnut* sp. nov. (2.73%) overlaps with divergence range between *L.* cf. *doughnut* and both *L. paradoxus* and *L. scottae* sp. nov. In this consideration, available molecular evidence remains inconclusive on whether *L.* cf. *doughnut* being distinct. As in *L. doughnut* sp. nov., genetic distances between *L.* cf. *doughnut* and both *C. coralliodytes* and

members of the "*Xynomaia sheni*" complex are substantial and beyond suggested inter-specific thresholds as addressed above: from *C. coralliodytes* (n = 2) by 9.25 ± 0.14% and from "*Xynomaia* species" (n = 10) on average by 9.40 ± 2.60%.

Given only one damaged specimen obtained and examined, we remain hesitant in drawing conclusion on identities of this form and pending further investigation on local cryptichirids, particularly those infesting the host coral *P. peroni*.

Lithoscaptus scottae sp. nov.

(Figures 3, 5F–H, 12, 13)

urn:lsid:zoobank.org:act:39F52BA7-2557-4B15-A35E-F4EF88A77E58

Material examined. Holotype ♀ (4.8 × 6.0 mm; CEL-Hapa-019/ASIZCR), Pak Lap Tsai, Sai Kung, 28 November 2019, on *Coelastrea aspera*); paratypes 2♀♀ (5.1 × 6.7 mm, 5.4 × 7.2 mm; CEL-Hapa-017, 018; SWIMS), 1♂ (2.9 × 4.7 mm; CEL-Hapa-015), same data as holotype. Other material: 5♀♀ (3.3 × 4.2 – 5.1 × 6.8 mm; CEL-Hapa-023-027), Long Ke Tsai, Sai Kung, 7–11 m, 28 November 2019, on *Favites pentagona*; 1♀ (4.7 × 6.5 mm; CEL-Hapa-028), 1♂ (3.0 × 5.0 mm; CEL-Hapa-029), Pak Lap Tsai, Sai Kung, 28 November 2019, on *F. pentagona*; 3♀♀ (4.6 × 6.2 mm–5.3 × 7.1 mm; CEL-Hapa-035-037), Pak Lap Tsai, Sai Kung, 28 November 2019, on *F. pentagona*.

Diagnosis. Carapace longitudinally ovate, anteriorly 2/3 depressed, deflexed, regions moderately defined, surface of isolated, well-separated rounded tubercles, gastric region laterally defined by oblique depression, meta-gastric region laterally each defined by two oblique grooves. Epistome medially elevated, laterally each of one longitudinal crest. Female thoracic sternum relatively narrow, medially depressed; anterior plate transversely rhomboid, 1.5 times as broad as long, surface punctated with low granules; sutures 4/5, 5/6, and 7/8 medially interrupted, suture 6/7 medially confluent of a short depression; sternite 7 medially of well-defined median line; gonopore on sternite 6 as an oblique slit, laterally sheltered by a narrow eave-like structure. Plp2 and Plp3 uniramous. Male thoracic sternum relatively broad, surface punctated, anteriorly arched; pleonal somites 3 to 6 each rectangular, lateral margins nearly parallel, telson two times as broad as long, semi-circular.

Description (based on holotype CEL-Hapa-019, female 4.8 × 6.0 mm). Carapace longitudinally ovate, 1.25 times longer than broad, broadest breadth, and most elevated at about 3/5 of CL; anterior 3/5 depressed, markedly deflexed and sculptured, sunken on hepatic region, which each of an oblique, broad groove, furnished with isolated, small rounded tubercles, giving an eroded texture, mesogastric region sparsely scattered with small conical spines, metagastric region laterally defined by two short deeply incised oblique grooves on each side, both grooves separated by raised granular cluster; posterior 1/3 inflated, outline arched, cardiac–intestine region broad of nearly 1/2 of cw, defined by the latter pair of abovementioned oblique groove, medially not connected, surface covered with numerous small, well-spaced, slightly elongated nodules for most of the length (Figure 12A). Front broad, inconspicuously convex, inner orbital angle of broad, convex, inflated lobe, dorsally lined with several small, rounded tubercles; exorbital angle crested, cristate, projecting beyond inner orbital lobes, confluent with anterolateral margin, which armed by series of small acute spines extending to approximately 1/3 of carapace length (Figures 12A, B). Pterygostmial region granular, rhomboid plate of which fused dorsally with carapace, suture inconspicuous but discernible (Figure 12B).

Basal plate of antennular peduncle longitudinally ovate, dorsally depressed, ventrally mildly convex, granular anteriorly armed with strong spines (Figures 12A, C). Eyestalk cylindrical, slightly elongated, nearly straight, extending anterolaterally, cornea extending beyond exorbital angle, basal to cornea lined with several small spinules dorsally (Figures 12A, C). Epistome medially elevated, laterally each of one well-defined longitudinal crest (Figure 12C). Mxp3 ischium depressed, surface rugose, mesial–distal lobe covered with numerous flattened granules, merus distal external lobe mildly produced, carpus slightly dilated; exopod as an elongated, bean-shaped plate (Figure 12D). Mxp1 endopod elongated-subtriangular, mesially convex (Figure 12F).

Cheliped symmetrical, merus to chela much compressed, carpus and palm dorsally lined with series of small spines; palm longer than fingers, dorsally punctate on external surface; fingers mildly compressed, tapering into fine chitinous tips (Figure 12I). P2 to P4 short and stout, meri compressed, carpi and propodi externally armed with spines or nodules (Figures 12J–L). P2 merus 1.7 times longer than broad, subquadrate, distal 1/4 armed with numerous small spines; carpus and propodus subequal in length, externally lined with series of acute teeth; dactylus claw-shaped, shorter than propodus (Figure 12J). P3 merus 1.4 times longer than broad, longitudinally ovate, distally of elongated nodules, posteriorly with small blunt spine; carpus and propodus externally of stout nodules; dactylus claw-shaped, shorter than propodus (Figure 12K). P4 merus 1.4 times longer than broad, longitudinally ovate, distally of elongated nodules; carpus and propodus externally lined with rounded nodules; dactylus claw-shaped, shorter than propodus, armed with small spinules along extensor margin (Figure 12L). P5 segments cylindrical, merus short, ovate, nearly unarmed; carpus and propodus elongated, subequal in length, laterally furnished with stout, rounded tubercles; dactylus slender, claw-shaped, tapering into an acute tip, curving and articulating ventrally (Figures 12M, N).

Thoracic sternite anteriorly extending reaching between bases of both Mxp3, anterior plate transversely rhomboid, 1.5 times as broad as long, anteriorly rimmed, surface punctated and furnished with low granules; constriction narrow, less than half of width of anterior plate, much depressed, medially grooved; sternites 5 and 6 not separated medially, strongly depressed, gonopore on sternite 6 as an oblique slit, laterally sheltered by a

narrow, eave-like structure; suture 6/7 medially nearly confluent, loosely connected by narrow transverse depression; sternite 7 medially depressed, median line deep, anteriorly separated from depression connecting sutures 6/7; suture 7/8 medially separated (Figure 12H). Plp1 to Plp3 uniramous (Figures 12O–Q).

Description of male (based on paratype CEL-Hapa-015, male 2.9 × 4.7 mm). Carapace 1.6 times as long as broad, longitudinally ovate, anterior 2/5 depressed, moderately deflexed, broadest breadth and most elevated at approximately 2/5 CL, overall granulation and delineation of regions far weaker than conspecific females; anterior part mildly sculptured, bearing a depression of inverted "V" shape, delineating a triangular mesogastric region, laterally subparallel with anterolateral region, floor of which finely granulated, sparsely scattered with isolated, slightly larger tubercles; frontal margin broad, nearly straight, laterally flanked by an elevated inner orbital lobe, which anteriorly armed with several slender, acute spines; exorbital angle triangular, anteriorly extending beyond inner orbital lobe, confluent with anterolateral margin, lined by a series of weak serrations, extending for 1/3 of carapace length; cardiac–intestine region vaguely defined by fine grooves, which barely discernible; posterior half of carapace inflated, scattered with small, low tubercles, roughly equally distant from one another (Figure 13A).

Basal plate of antennular peduncle outline narrow-triangular in dorsal view, anteriorly armed with several acute teeth, mesial margin basally of small raised longitudinal lobe and scattered with small spinules on dorsal surface (Figure 13A). Eyestalks short and stout, oriented anterolaterally, cornea spheroidal, slightly expanded (Figure 13A).

Cheliped symmetrical, robust, slightly larger in size than other pereiopods, merus short and stout, prismatic; carpus longitudinally ovate, dorsally spinose; chela palm slightly inflated, externally punctated, spinose along dorsal margin; fingers stout, shorter than palm, mildly deflexed (Figure 13B). P2 to P4 short and robust, inconspicuously decreasing in robustness; P2 armed with numerous spinules externally on merus to propodus (Figure 13C), P3 and P4 meri to propodi externally granular, dactyli slender, curved mesially; P5 slender, unarmed, longer than P4, propodus and dactylus articulating ventrally (Figure 13D).

Thoracic sternite anteriorly extending between bases of both Mxp3, broader and less as sculptured as in conspecific females; anterior projection broader than long, anteriorly arched, smoothly rimmed, surface sparsely punctated, sternites 5 and 6 medially depressed, not separated medially; sternite 7 anteriorly separated from sternite 6 by deep U-shaped suture, medially divided by well-defined median line; sternite 8 separated into two triangular plates by posterior emargination, on each side perforated by gonopore (Figure 13E). Pleon slender, lateral margins from somites 3 to 6 nearly confluent, parallel, each somite quadrate, broader than long; telson broader than long, semi-circular (Figure 13F). G1 dorsal-ventrally compressed, slender, blade-like, tapering into a fine tip, external margin lined with about 15 stiff, isolated, roughly evenly-spaced setae (Figures 13G, H). G2 short, slender, merely 1/4 length of G1, distally dilated (Figure 13I), *in situ* briefly inserted into base of G1.

Host coral. So far, local material was retrieved from *C. aspera* and *Favites pentagona* of the Merulinidae. Host sharing was observed on *C. aspera* with *X. sheni* (see below).

Etymology. The present species is named after Dr. Paula J. B. Scott, author of *The Corals of Hong Kong* (1984). This researcher, an expert of coral-associated invertebrates, witnessed the abrupt decline of coral communities in Hong Kong during the 1980s (Scott and Cope, 1982; Scott and Cope, 1990). Her pioneer, thorough and reader-friendly book laid foundation for the current understanding of the local scleractinian fauna.

Type locality. Pak Lap Tsai (白鱲仔), Sai Kung, Hong Kong.

Geographical distribution. So far recorded from only two sites, both coral communities in eastern waters of Hong Kong: Pak Lap Tsai, and Long Ke Tsai (浪茄仔) (see Figure 1). Considering the broad, Indo-Pacific distributional range of both host species (see Dai and Horng, 2009), potentially broader distribution of *Lithoscaptus scottae* sp. nov. is anticipated.

Remarks. The present species is recognized as closely related to, but distinct species from, *L. paradoxus* based on the three lines of evidence, namely, host records, morphological examination, and molecular analyses.

Among the other 10 previously described congeners, although all largely infesting hosts of the Merulinidae, preference of *L. scottae* sp. nov. only overlaps with that reported for *L. hellerii*. In the literature, hosts of *L. hellerii* include *Astrea curta* (as *Montastrea vacua*), *C. aspera* (as *F. spectabilis*), *Dipsastraea pallida*, *D. speciosa*, *Favites chinensis*, *F. flexuosa*, *F. pentagona*, *F. valenciennesii*, *Goniastrea stelligera*, and *Goniastrea* sp. (Fize and Serène, 1957; Takeda and Tamura, 1981a; van der Meij and Nieman, 2016). *Lithoscaptus scottae* and *L. helleri*, however, are nevertheless morphologically and genetically distinct.

Females of *L. scottae* sp. nov. can be distinguished from those of *L. paradoxus* by the following features: (1) contours of carapace, *L. scottae* sp. nov. most elevated at approximately 2/3 of CL (Figure 12B), whereas that of *L. paradoxus* at near mid-length (Figure 9B); (2) sculpturing of dorsal surface of carapace, that of *L. scottae* sp. nov. more markedly sculptured metagastric region, which laterally defined by two pairs deep, broad oblique grooves, whereas cardiac–intestine region relatively poorly defined laterally (Figures 5F, G, 12A), in comparison with *L. paradoxus*, which metagastric region not delineated by deep grooves, and cardiac–intestine region delimited by rather deep and narrow grooves (Figures 5B, C, 9A); and (3) anterior

extension of thoracic sternite, that of *L. scottae* sp. nov. markedly broader than long (Figure 12H) compared with *L. paradoxus* merely as long as broad (Figure 9H).

Assessed based on illustrations provided in various published accounts, females of *L. scottae* sp. nov. can be distinguished from the other congeners by: (1) contour of carapace when viewed laterally, in *L. scottae* sp. nov. anterior 3/5 of carapace strongly deflexed (Figure 12B), instead of less than half as in *L. pacificus* [fig. 2b in Edmondson (1933)], roughly half as in *L. pardolatus* [fig. 1b in Kropp (1995)] and *L. doughnut* sp. nov. (Figure 10B), mildly deflexed as in *L. prionotus* [fig. 4b in Kropp (1994)]; (2) sculpturing on anterior part of carapace, in *L. scottae* sp. nov., well defined by broad, shallow depressions (Figures 5F, G, 12A), in contrast with oblique depression behind inner orbital lobe of *L. helleri* deep and prominent [fig. 24 in Fize and Serène (1957); text-fig. 2A in Takeda and Tamura (1981a)], likewise deep, and laterally defining metagastric region in *L. prionotus* [fig. 4a in Kropp (1994)], that of *L. tuerkayi*, likewise deep and prominent [fig. 1A in van der Meij (2017)], whereas as two short longitudinal grooves lateral to metagastric region as in *L. doughnut* sp. nov. (Figure 10A); (3) armature of carapace, in *L. scottae* sp. nov. anterolateral margin entire, lined with small spines, inner orbital lobe anteriorly rounded, dorsally raised and nearly smooth, and mesogastric region covered with isolated, small tubercles (Figure 12A), in contrast to that interrupted at about 1/5 of CL as in *L. grandis* [fig. 1A in Takeda and Tamura (1983)], or armed with strong, acute or conical teeth along anterolateral margin, inner orbital lobe anteriorly armed, and mesogastric region markedly spinose: *L. grandis* [fig. 1A in Takeda and Tamura (1983)], *L. nami* [figs. 5G, 7A in Fize and Serène (1957)], *L. pardolatus* [fig. 1a in Kropp (1995)], *L. prionotus* [fig. 5a in Kropp (1994)], *L. tuerkayi* [fig. 1A in van der Meij (2017)], *L. tri* [figs. 5H, 8A in Fize and Serène (1957); text-fig. 2A in Takeda and Tamura (1980)]; (4) Mxp3 ischium roughly as long as broad in *L. scottae* sp. nov. (Figure 12D), while much broader than long in that of *L. tuerkayi* [fig. 1C in van der Meij (2017)], or longer than broad in *L. tri* [fig. 9A in Fize and Serène (1957); text-fig. 2B in Takeda and Tamura (1980)]; (5) P5 carpus and propodus laterally tubercular in *L. scottae* sp. nov. (Figure 12N) while that of *L. semperi* nearly smooth [fig. 1J in van der Meij (2015b)]; and (6) anterior plate of female thoracic sternites broader than long in *L. scottae* sp. nov., with constriction narrow, less than half of width of anterior plate (Figure 12H), which nearly as long as broad in *L. prionotus* [fig. 4c in Kropp (1994)], and transversely sub-octagonal in *L. doughnut* sp. nov., and constriction broader (Figure 10H). In addition, telsons of male *L. scottae* are semi-circular, much broader than long (Figure 13F), can be distinguished from *L. grandis* [fig. 1d in Takeda and Tamura (1983)] and *L. pacificus* [fig. 2j in Edmondson (1933)], which are rounded-triangular for both species.

As addressed above, the material of the present form (n = 14) does not cluster at intra-specific level with any COI reference sequences available on GenBank, but as shown in NJ tree in Figure 6B, exhibiting closest affiliation to *L. paradoxus*, which voucher specimens from Indonesia (KU041825.1; mean K2P distance 4.25 ± 0.65%), and Guam (KU041820.1; K2P distance, 4.65 ± 0.56%), both specimens collected from hosts of *Platygyra* species. These divergence values between *L. scottae* sp. nov. and *L. paradoxus* are moderate within range of interspecific values of thoracotreme crabs (1.49%–6.25%) and even exceed the lowest value between described *Lithoscaptus* species (*L. helleri* and *L. tuerkayi*) at 3.57%, thus supporting both being distinct. Our material is also genetically distinct from all other congeneric species by a larger extent: ranging from 5.80% from *L. prionotus* (KJ923664.1, KJ923665.1; 5.80 ± 0.48%), 12.05% from *L. helleri* (KU041819.1; 11.05 ± 0.50%), to 12.73% from *L.* cf. *helleri* (KU041824.1; 12.73 ± 0.39%). *Lithoscaptus scottae* sp. nov. is also distinct from the undescribed forms referred as sp. A (KU041828.1; mean distance, 6.33 ± 0.59%), sp. C (KU041827.1; mean distance, 7.50 ± 0.72%), sp. D (KU041823.1; mean distance, 6.23 ± 0.71%) and sp. Z (KU041830.1; mean distance, 6.25 ± 0.82%). Precise figures are provided in Table 1.

Xynomaia sheni Fize and Serène, 1956 species complex

(Figures 4E, F, 5I, J, 14, 15C)

Troglocarcinus sheni Fize and Serène, 1956b: 380, fig. A.

Troglocarcinus (*Troglocarcinus*) *sheni*—Fize and Serène, 1957: 74, figs. 11G, 16, 17A–E, 20C, D, pls. 4(3, 4), 5(5, 6), 12B, 15A–D.

Pseudocryptochirus sheni—Serène, 1968: 398.

Hiroia sheni—Takeda and Tamura, 1981b: 20.

Xynomaia sheni—Kropp, 1990: 446, fig. 15.—Ng and Davie, 2002: 380.—Paulay et al., 2003: app.—van der Meij and Reijnen, 2014: app. 1.—van der Meij and Nieman, 2016: app. 1.

Material examined. 5♀♀ (2.3 × 3.1 mm – 3.9 × 5.4 mm; CEL-Hapa-001–005), Long Ke Tsai, Sai Kung, 7–11 m, 26 November 2019, on *C. aspera*; 1♀ (3.2 × 4.5 mm), Pak Lap Tsai, Sai Kung, 28 November 2019, on *C. aspera*.

Diagnosis. Carapace longitudinally ovate, longitudinally and laterally convex, anteriorly of small conical spines grading into isolated rounded tubercles on the posterior half, regions mildly defined, gastric region laterally defined by shallow depression behind orbit. Basal antennular segment armed with small anterolateral spine; epistome of three longitudinal crests. Female sternum relatively broad, median depression shallow; anterior plate transversely ovate, surface coarsely punctated; sutures 4/5, 5/6, and 7/8 short, medially interrupted, sternite 7 medially of well-defined median line; gonopore on sternite 6 as an oblique slit, laterally sheltered by a narrow eave-like structure. Plp2 and Plp3 uniramous.

Description (based on CEL-Hapa-002, female 3.5 × 4.8 mm). Carapace longitudinally ovate, 1.4 times longer than broad, mildly convex longitudinally and transversely, broadest and most elevated at approximately half of CL; anteriorly half densely furnished with stout, conical spines, roughly evenly-spaced, replaced by rounded granules posteriorly; front broadly concave, anteriorly lined with three slender spines, inner orbital lobe broad, inflated, anteriorly armed with numerous strong, elongated spines; exorbital angle spinose, confluent with anterolateral margin, which raised, marginally stout, armed with series of strong spines, lateral to eyestalks furnished with short, oblique deep groove; hepatic region behind each inner orbital lobe markedly depressed, region of which invert-triangular, floor likewise of stout conical spines, anteriorly defining mesogastric region; mesogastric region broadly triangular, moderately inflated, likewise of conical spines; cardiac–intestine region delineated by two shallow longitudinal depressions anteriorly, laterally barely defined; mesobranchial region lined with shallow longitudinal groove (Figures 14A, B). Pterygostomial region granular, rhomboid plate of which incompletely fused with carapace, suture visible (Figure 14B).

Basal plate of antennular peduncle elongated fang-shaped in outline, sub-cylindrical, dorsally strongly spinose, ventrally inflated, granular (Figures 14A, C, D). Second antennal segment armed with lateral spine distal externally (Figures 14C, D). Eyestalk short and stout, cornea slightly expanded, basal of which scattered with several small spinules on dorsal surface (Figure 14D). Epistome medially elevated as a distinguishable longitudinally crest, lateral to which each bearing one distinct longitudinal crest, all extending to anterior margin of epistome (Figure 14C). Mxp3 ischium depressed, finely granular, medial margin nearly straight, merus distal–externally not produced, carpus slightly dilated along internal margin; exopod as a small, elongated ovate plate (Figure 14E). Mxp1 endopod elongate-triangular (Figure 14G).

Cheliped symmetrical, slightly reduced in size; carpus and palm dorsally lined with small blunt spines; palm mildly inflated, externally smooth, fingers not gapping, weaking deflexed, relatively stout, tapering into fine chitinous tips (Figure 14J). P2 to P4 short and stout, meri much compressed, meri to propodi externally armed with projections, dactyli slender, much curved, each tapering into a fine tip (Figures 14K–M). P2 merus elongated sub-pentagonal, 1.8 times as long as broad, anteriorly lined with weak spinules, distally of numerous stout spines; carpus and propodus externally of numerous acute spines (Figure 14K). P3 merus longitudinally ovate, 1.3 times longer than broad, distally of numerous stout nodules; carpus and propodus cylindrical, subequal in length, externally lined with series of stout nodules (Figure 14L). P4 merus longitudinally ovate, 1.3 times as long as broad, distally of several stout, blunt spines; carpus and propodus cylindrical, subequal in length, externally lined with series of blunt spines (Figure 14M). P5 slender and elongated, segments cylindrical; merus subquadrate, 1.4 times as long as broad, distally armed with low tubercles; carpus and propodus subequal in length, laterally armed with rounded spines, mesially smooth; dactylus shorter than propodus, laterally spinose, curving and articulating ventrally (Figures 14N, O).

Thoracic sternite anteriorly extending reaching between bases of both Mxp3; anterior plate transversely ovate, anteriorly rimmed, lateral portion slightly swollen, surface coarsely punctated; constriction broad, more than half of width of anterior plate, faintly grooved among midline; sternites 5–7 mildly depressed mesially; sutures 4/5, 5/6, not 6/7 separated mesially; gonopore on sternite 6 obliquely ovate, partially exposed when viewed ventrally, laterally sheltered by narrow eave-like structure; sternite 7 medially separated by well-defined median line (Figure 14I). Plp1 to Plp3 uniramous.

Host coral. Six female individuals have been found on colonies of *C. aspera*. Five individuals (CEL-Hapa-001 to 005) were recovered from the same colony (Figures 4E, F); one individual (CEL-Hapa-016) was found to be sharing the same host with *Lithoscaptus scottae* sp. nov. (CEL-Hapa-015, 018, 019). The host of *X. sheni* recorded in the literature include *Pectinia lactuca*, *P. paeonia*, and *Mycedium elephantotus* of the Merulinidae (Budd et al., 2012; Huang et al., 2014), and *Oxypora lacera*, the Lobophylliidae (Fize and Serène, 1956b; Fize and Serène, 1957; Kropp, 1990; van der Meij and Reijnen, 2014; van der Meij and Nieman, 2016). See *Remarks* below.

Type locality. Nha Trang, Vietnam.

Geographical distribution. Eastern Indian Ocean to West Pacific: Phuket, Thailand (Ng and Davie, 2002); Lembeh Strait and Sumatra, Indonesia (Serène, 1968; van der Meij and Nieman, 2016), Semporna, Malaysia (van der Meij and Reijnen, 2014), Nhatrang, Vietnam (Fize and Serène, 1956b; Fize and Serène, 1957), Hong Kong, South China (this report), Mariana Islands (Paulay et al., 2003), and Guam (Kropp, 1990) (but see *Remarks* below).

Remarks. Currently, three species have been placed under *Xynomaia* Kropp, 1990, namely, *X. boissoni* (Fize and Serène, 1956a), *X. sheni*, and *X. verrilli* (Fize and Serène, 1957); the genus is characterized by carapace not anteriorly deflexed, dorsally furnished with a W-shaped depression on the anterior portion, pterygostomian region not fused dorsally with carapace, antennal segment 2 distally armed with lateral spine, and P2 merus lacking disto-mesial projection (Kropp, 1990). All of these three species were described based on material from Nhatrang, southern Vietnam, all under *Troglocarcinus* [in Fize and Serène (1957) as *T.* (*Troglocarcinus*) *boissoni*, *T.* (*T.*) *sheni*, and *T.* (*Favicola*) *verrilli*]. Apart from host differences, the three species can be differentiated by outline and spinulation on carapace (see Fize and Serène, 1957). Unfortunately, relevant type lots were not re-examined or further reported so far. *Xynomaia sheni* was further reported from Guam by Kropp (1990) and selected as type species of *Xynomaia*. Several later reports under this name from the West Pacific contributed gene sequences (see below),

but associated morphology remains yet illustrated in detail. *Xynomaia boissoni*, symbionts of the Merulinidae and Lobophylliidae, was later reported from (1) Honshu, Japan (Takeda and Tamura, 1983; Takeda and Tamura, 1985), yet as admitted by these authors, "lateral border of carapace in the specimens in hand is reasonably less convex than in the original figure" (p. 8, 1983) and (2) New Caledonia by Richer de Forges and Ng (2006), who provided no elaborations or illustrations. *Xynomaia verrilli*, symbiont of *Oulophyllia crispa* (as *Platygyra gigantea*), *Dipsastraea speciosa* (as *Favia speciosa*), both Merulinidae, a rare species at the time of description, was never reported elsewhere since.

Our local material consists of six female specimens identifiable as *Xynomaia*, among which only two were relatively intact: CEL-Hapa-002 (illustrated as Figure 14) and 004 (not dissected), differing slightly by overall shape of carapace (Figures 5I, J). Compared with illustrations of the original material provided by Fize and Serène (1957), we tentatively identify the local form as *X. sheni*, given the following morphological features: (1) relative broad width between bases of both orbits in dorsal view and (2) depression on anterior half of carapace and longitudinal groove laterally defining cardiac–intestine region shallow. However, several features differ, namely, (1) convexity of lateral margin or carapace—mildly arched in our material while much convex in the type material; (2) carapace dorsally furnished with larger rounded tubercles on posterior half while less as tubercular as in the types; (3) mesobranchial region furnished with shallow longitudinal groove, while such groove is absent in types (Figures 5I, 14A *vs*. fig. 16 in Fize and Serène, 1957); and (4) outline of ambulatory meri, in comparison with the type material, that of P2 more elongated in CEL-Hapa-002, while all short and stout as in P3 to P5 (Figures 14K–N *vs*. fig. 11G in Fize and Serène, 1957).

Molecular evidence as shown in the NJ tree of COI sequences (Figure 6B) concerning this poorly known genus is perplexing. First, COI reference sequences from GenBank labeled as "*X. sheni*" (KJ923679.1, KJ923680.1, and KU041817.1) are clearly not conspecific: KJ923679.1 and KJ923680.1 both from Semporna, Borneo, Malaysia share a same haplotype but of different host families (*Pectinia lactuca* and *Mycedium elephantotus* of the Merulinidae), but these two sequences differ from KU041817.1 (Kropp's material from Guam) by a K2P distance of 14.97%. Sequences extracted from the Guam specimen as *X. sheni* (KU041817.1; shorter length of 396 bp) and another as *X.* sp. from Lembeh Strait, Indonesia (KU041835.1; 625 bp), after alignment, are identical throughout the 396 bp; thus, K2P distance is calculated to be 0 and very probably share the same COI haplotype. These two specimens were from hosts of different families (*Pectinia paeonia*, Merulinidae, and *Oxypora lacera*, Lobophylliidae, respectively). The Malaysian haplotype (KJ923679.1, KJ923680.1) was shown to nest among various *Lithoscaptus* species in reconstruction presented by van der Meij & Reijnen (2014; also Figure 6B). In this aspect, whether or not either of these two haplotypes represents the true *X. sheni* cannot be ascertained.

A close examination of our material probably stir up another aspect of enigma: substantial species-level genetic differentiation and conservative morphologies among sympatric individuals. The six individuals belong to two lots, both from host *C. aspera*, with CEL-Hapa-001 to 005 on the same colony and 016 on another, the latter sympatric with *L. scottae* sp. nov. From the same colony with domicile openings merely centimeters apart (Figure 4F), three distinct haplotypes are retrieved (CEL-Hapa-001-003, CEL-Hapa-002, and CEL-Hapa-004-005-016). The latter haplotype (004-005-016) corresponds to that from Guam and Indonesia (KU041817.1, KU041835.1) mentioned above. Genetic distances between 001-003 and 004-005-016 (4.83%), and 002 and 004-005-016 (4.13%), are substantial to be recognized as interspecific divergences among cryptochirid (Figure 7) and other thoracotreme crabs (1.49%–6.25%; see above).

Difficulties in the morphological identification of this genus have been notorious. Small body sizes, and morphological features previously considered to be diagnostic (see Kropp, 1990) being probable results of convergent evolution, attribute to a "composite" *Xynomaia* in the phylogenetic reconstruction presented by van der Meij and Nieman (2016). At specific level, evidence of genetic differentiation suggests specific differentiation, while morphologies remain conservative, which might indicate occurrences of cryptic and sympatric speciation events. Reluctantly, we remain to identify the present genetically distinct forms as *X. sheni* species complex, noting its unusual genetic divergence and plasticity in host preferences. Deciphering true identities of *X. sheni*, however, might require examination of type or topographic material, which currently remains unresolved. Genetic and species diversity of this "*X. sheni* complex," anyhow, can be further elucidated with accession to fresh material, hopefully made possible in the near future.

Discussion

Sequence divergence and species identifications of cryptochirid crabs

Molecular approaches adopted in species identification in the present study comprises two aspects, namely, phylogenetic relationships and pairwise distance between query and reference sequences. Results of both approaches are respectively indicated as Figures 6, 7. In contrast, as shown in Figures 6A, B, precise identification was reached in one species using 16S rDNA sequences, whereas precise identification was reached in all five (of six OTUs) by COI sequences (see also elaborations above). This differing resolution in species identification of the two adopted gene markers can at least be partially attributed to

the 16S rDNA marker being slightly conserved than that of COI. This had been demonstrated in studies on various groups of decapod crustaceans, particularly among "young" species in rapidly evolving lineages, such as freshwater (e.g., Shih et al., 2007; Yeo et al., 2007) and intertidal crabs (Shih and Suzuki, 2008; Shih et al., 2010; Ragionieri et al., 2012). The discrepancy is likewise observable among cryptochirids as herein reported. Moreover, this is compounded by the current number of available sequences in the depository of GenBank. As of September 2022, for 16S rDNA, over 150 reference sequences representing 18 species (including two of tentative generic identification) were available, in comparison to over 380 of 43 species (including nine of tentative generic identification) for COI. In this consideration, COI remains to be an informative source as a genetic marker for species identification and barcoding analyses. In the present study, while the 16S rDNA marker shows inadequate resolution in species delimitation, that of COI corresponds well with morphological delineations.

Despite the lack of resolution in revealing phylogenetic relationships between deeper lineages, as demonstrated by van der Meij and Nieman (2016) on cryptochirids, the variability of the mitochondrial COI marker makes it useful for species identification and frequently used in barcoding analyses, and genetic (K2P) distances (maximum intraspecific and minimum interspecific genetic distances) may be useful for considerations in species delimitation (see e.g., Bucklin et al., 2011; Chu et al., 2015 for reviews). Based on query and reference sequences, we report mean intraspecific K2P distances of cryptochirids being 1.06 ± 0.76% and interspecific (intrageneric) distance at 7.16 ± 3.27%. Genetic distances among described *Lithoscaptus* species vary from 3.57% to 14.97%. Among described species of *Lithoscaptus*, lowest pairwise distance was observed between *L. tuerkayi* (KU745732.1) and *L. hellerii* (KU041819.1) at 3.57%. These values have been taken into consideration in species delimitations. These values are comparable with threshold values previously reported for thoracotreme crabs (1.49%–6.25%), from studies of groups in which taxonomy is relatively well resolved, and the examined taxa show discrete morphologies (see Davie et al., 2010; Shih et al., 2012, 2019; KJH Wong et al., 2012). However, cryptochirid taxonomy is nowhere well resolved in two sense: numerous previously unrecognized species-level taxa (Wei et al., 2016; Bähr et al., 2021; Xu et al., 2021; see below) and previous morphology-based generic placement insufficient in encapsulate true species richness, thus rendered composite (van der Meij and Nieman, 2016; see *Remarks* under *L. doughnut* above). As such, both our intra- and interspecific distance values show considerable range of variation and are probably inflated. Adopting relevant threshold values for species delimitation might require alterative lines of supporting evidence. Nevertheless, the NJ tree constructed based on COI sequences (Figure 6B) resulted in similar topology with that by van der Meij and Nieman (2016), likewise showing morphologically resembling *Cryptochirus*, *Fungicola*, *Pelycomaia*, and *Xynomaia* nested within. *Lithoscaptus helleri* and *L. tuerkayi* are probably aberrant members of the genus. This genetic marker does not foster resolution in resolving phylogenies of deeper lineages (see Chu et al., 2015), thus pend for further sampling of molecular data, and taxonomic revisions of, especially, *Lithoscaptus* and related groups.

Neglected symbionts of the scleractinian fauna: Case study of Hong Kong

The scleractinian fauna of Hong Kong, as a historical parallel of local records of brachyuran crabs (see historical account under preparation by KJHW, BKKC, and colleagues), has been recorded since the mid-nineteenth century, both as a subsets of findings resulted from the North Pacific Exploring Expedition (1853–1856). The scleractinian fauna recorded during this expedition was reported by Verrill (1866), including 10 species from seas in the vicinity of Hong Kong (see Tam and Ang, 2008). The current understanding of the local scleractinian fauna had its foundations in the 1980s by Veron (1982) and Scott (1984), the latter a well-illustrated guide book mentioned above. By 2005, a revised guide book by Chan et al. (2005) reported 84 scleractinian species. During the recent decades, local shallow-water coral communities of Hong Kong have been routinely surveyed by researchers (e.g., KT Wong et al., 2018; Yeung et al., 2021a) and amateur divers as an environmental education program (Cheang et al., 2017), and the scleractinian inventory has been reasonably well established.

In comparison with the rather detailed reports of corals, cryptochirid crabs have been poorly documented in the literature. The first record of a cryptochirid crab from Hong Kong was published by Shen (1936), in which *C. hongkongensis* Shen, 1936 [now *Neotroglocarcinus hongkongensis* (Shen, 1936)] was described, while its host, precise locality, and deposition of types remained unspecified. Shen (1940), in compiling a checklist of brachyuran fauna of Hong Kong, included records of only two males and two females with no indication of their type status, listed as "No. 12799," probably the catalog number of the material deposited at the Fan Memorial Institute of Biology, Peiping, the whereabouts and status of which are currently unknown. This species was subsequently considered synonymous with *P. viridis* Hiro, 1938 by Utinomi (1944). In deciphering identities of *C. hongkongensis*, Kropp (1988b) showed that both species are distinct and, based on the available material in various institutes, deduced that the host of *N. hongkongensis* should probably be *Duncanopsammia peltata*. This species remained the single host of cryptochirids recorded from Hong Kong, until van der Meij (2012), based on image of a crescent-shaped domicile opening on *Turbinaria mesenterina* presented by Scott (1984) (Fig. 42B), reported *P. viridis*. The latter record might not be as affirmative, as the

photographed domicile might instead belong to *Neotroglocarcinus dawydoffi* (Fize and Serène, 1956a) instead (SET van der Meij, pers. comm.). We have not yet acquired a local material of any these two (or three?) recorded species. This bold asymmetry in the understanding of the local scleractinian and cryptochirid fauna is highlighted by the surprising addition of five gall crab species in this study, based on a limited material that was amassed during several days of intensive samplings. This asymmetry is likewise apparent among faunal records in the vicinity of South China: a scleractinian fauna of 315 species (Zou et al., 2008; excluding records from only Taiwan and East China Sea) while only three cryptochirid species reported (Yang et al., 2008). This can be partly attributed to the group being intuitively "cryptic" symbionts of scleractinians, easily overlooked among coral communities, a habitat generally poorly surveyed, difficult in sampling, and lack of taxonomic expertise. In this sense, the number of cryptochirids so far recorded from Hong Kong and the South China appears to be an underestimation.

Dichotomous key of female cryptochirid crabs of Hong Kong

As sampling in Hong Kong cannot be considered exhaustive at present, we refrain from providing a key based on the sampled coral hosts. Female individuals of cryptochirid species so far reported from Hong Kong can be identified by the key below:

1a. Carapace depressed, vast-shaped, broadest posterior to mid-length; P2 merus distal-dorsally dilated laterally beyond articulation with carpus—**2 Genera *Neotroglocarcinus* and *Pseudocryptochirus***

1b. Carapace moderately or marked inflated, overall longitudinally ovate or subquadrate; P2 merus distal-dorsal angle not dilated—**3 Genera *Cryptochirus*, *Lithoscaptus*, and *Xynomaia***

2a. Anterior plate of thoracic sternum lined with one transverse row of tubercles—***Neotroglocarcinus hongkongensis* [recorded hosts: *Turbinaria mesenterina*, *T. nidifera*, and *Duncanopsammia peltata*]**

2b. Anterior plate of thoracic sternum nearly smooth—***Pseudocryptochirus viridis* [recorded hosts: *Turbinaria frondens*, *T. mesenterina*, *T.* cf. *patula*, *T. reniformis*, and *T. stellulata*]**

3a. Carapace moderately inflated but not anteriorly deflexed (Figure 14B); antennal segment 2 distally armed with lateral spine (Figure 14D)—***Xynomaia sheni* species complex [local host: *Coelastrea aspera*]**

3b. Carapace anteriorly deflexed—**4**

4a. Mid-portion (gastric region) of carapace furnished with rounded cluster densely set rounded tubercles, regions strongly sculptured (Figures 5A, 8A)—***Cryptochirus coralliodytes* [local host: *Platygyra acuta*]**

4b. Mid-portion of carapace sparsely lined with small conical spines, regions moderately indicated—**5**

5a. Anterior plate of thoracic sternum about as long as broad (Figure 9H)—***Lithoscaptus paradoxus* [local hosts: *Platygyra acuta* and *P. contorta*]**

5b. Anterior plate broader than long—**6**

6a. Carapace most elevated at about 2/3 carapace length (Figure 12B), gastric region lined with two broad oblique grooves (Figures 5F, G, 12A); anterior plate of thoracic sternum transversely ovate (Figure 12H)—***Lithoscaptus scottae* sp. nov. [local hosts: *Coelastrea aspera* and *Favites pentagona*]**

6b. Carapace elevated at about half mid-length (Figure 10B), gastric region laterally each defined with short concave groove (Figures 5D, 10A); anterior plate of thoracic sternum distinctly octagonal, broader than long (Figure 10H)—***Lithoscaptus doughnut* sp. nov. [local host: *Plesiastrea peroni*]**

Is the form of female thoracic sternum a species-level diagnostic character?

Morphologies such as dorsal surface of carapace, and lateral surfaces of ambulatory legs, are often subjected to intense abrasion and wear, thus the substantial variation. Alternatively, the taxonomic value of the form of thoracic sternites, being a "non-external" morphological feature, has been demonstrated for female cryptochirids. While the form of sutures 4/5 to 7/8 (whether medially confluent or separated) is comprised of three patterns, warranting delineation of respective subfamilial grouping (Guinot et al., 2013), the form of the anterior plate (sternite 3, anterior to base of P1), in terms of outline and surface ornamentation, has been used by Kropp in the delineation of *Opecarcinus* species (Kropp, 1989) and the distinction between Pacific genera (Kropp, 1990). In this consideration, we attempted to employ this character among *Lithoscaptus* species. Among previously described species (n = 10), however, thoracic sternites of only three were illustrated: *L. paradoxus* [fig. 4c in Kropp (1988a)], *L. prionotus* [fig. 4c in Kropp (1994)], and *L. tuerkayi* [fig. 4B in van der Meij (2017)]. Both of the two new species described in this study have a structure that differs markedly from those illustrated earlier (see *Remarks* under each species). As such, we propose the inclusion of the form of female thoracic sternites, particularly the shape and surface texture of the anterior plate, as diagnostic features of *Lithoscaptus*-related taxa. Further documentation of this structure from the relevant material would test its viability in species-level identifications.

Broad host range, or unrevealed diversity?

Based on our material from Hong Kong of at least five species, each was found symbiotic with one to two host species.

Lithoscaptus doughnut sp. nov. (and *L.* cf. *doughnut*) were retrieved from hosts of *P. peroni* of the Plesiastreidae, a family previously not reported to host cryptochirid crabs. The four remaining species largely infest the hosts of Merulinidae. Local host records of *C. coralliodytes* and *L. paradoxus* overlap with data from published sources but not for *X. sheni*. The Hong Kong material of *C. coralliodytes* from the present study was collected from *P. acuta*, while 10 genera of the hosts had been recorded in the literature: *Hydnophora* (Red Sea), *Leptastrea* (Leptastreidae; Red Sea), *Leptoria* (Minicoy Island), *Platygyra* (Vietnam, Borneo, West to Central Pacific), *Trachyphyllia* (Philippines), *Goniastrea* (Philippines, Palau, Vietnam, Taiwan), *Paragoniastrea* (Taiwan), *Merulina* (Ryukyus and Ogasawara), *Coelastrea* (Palau), and *Dipsastraea* (Hawaii, Palau) (Semper, 1881; Borradaile, 1902; Potts, 1915; Hiro, 1937; Fize and Serène, 1957; Takeda and Tamura, 1980; Kropp, 1988a; Wei et al., 2006; Figure 15A). *Lithoscaptus paradoxus* in Hong Kong was collected from two species of *Platygyra*, while recorded hosts include taxa of six genera, including *Cyphastrea* (Vietnam), *Dipsastraea* (Vietnam), *Favites* (Vietnam), *Goniastrea* (Vietnam, West Pacific), *Paragoniastrea* (Taiwan), and *Platygyra* (Vietnam, Celebes Sea, Cook Islands) (Fize and Serène, 1957; Kropp, 1988a; Wei et al., 2006; van der Meij and Nieman, 2016; Figure 15B). The material of *L. scottae* sp. nov. was retrieved from *C. aspera* and *Favites pentagona*, both genera previously reported to be hosts of cryptochirids (*C. aspera*: *C. coralliodytes*; *F. pentagona*: *L. paradoxus*, *L. helleri*). The Hong Kong material identified as *X. sheni* was retrieved from only *C. aspera*, while recorded hosts in the literature include *Pectinia* (Borneo, Guam) and *Mycedium* (Borneo) of the Merulinidae, and *Oxypora* (Sulawesi) of the Lobophylliidae (Fize and Serène, 1957; Kropp, 1990; van der Meij and Reijnen, 2014; van der Meij and Nieman, 2016; Figure 15C). Such diversity of hosts among different geographical regions may be attributed to variation in sampling effort. Further samplings should be conducted to reveal the host usages of cryptochirid crabs in the Indo-Pacific region.

Among the over 40 Indo-Pacific species, most (n = 37) show a narrow range of one to two host genera. Given the above observations, can we reach the conclusion that, in terms of host range, *C. coralliodytes* and *L. paradoxus* are "generalist" along a generalist–specialist gradient? Patterns of host specificity can be confounded by unrecognized diversity. Recent investigations on *H. marsupialis*, a species distributed from western Indian Ocean to the Central Pacific (Wei et al., 2016; Bähr et al., 2021), showed important implications. Despite highly conserved morphologies, genetic data based on materials amassed across the distribution range recognize multiple putative species, each biologically distinct (COI divergences range from 3.2% to 15.7%; Bähr et al., 2021), and putative species differ in recorded host (of *Pocillopora*, *Seriatopora*, and *Stylophora*; Wei et al., 2016; Bähr et al., 2021) and early larval characters (Gore et al., 1983). A similar pattern is also observed among *Opecarcinus* species by Xu et al. (2021), who showed the current taxonomic understanding (of nine species; Kropp and Manning, 1987; Kropp, 1989) being a gross underestimation of true diversity (at least 25 OTUs). Both cases illustrate another aspect of "crypticity," revealing a discrepancy between the current species inventory and unrecognized true diversity of species or OTUs. Previously presumed "generalist" niches (as assessed by host range) are confounded by poor taxonomic resolution, where biologically distinct OTUs are examined to be undifferentiated. Additionally, for past records of *Cryptochirus* and *Lithoscaptus*, the ambiguity had been compounded by a confusing taxonomic history. These two genera, for many decades, had been placed as synonyms and collectively referred as symbionts of massive "Faviidae" corals. This was satisfactorily resolved merely 30 years ago (see Kropp, 1988a). For the 12 host genera of *C. coralliodytes* and *L. paradoxus* enumerated above, also *Plesiastrea*, the host of *L. doughnut* sp. nov., shows very broad Indo-Pacific distribution ranges (see e.g. Veron, 2000; Huang et al., 2014), and the presence of previously unrecognized cryptochirid taxa is certainly anticipated. As obligate symbionts, the biology of cryptochirids is highly dependent on that of their hosts (e.g., Hiro, 1937; Utinomi, 1944). Assessing any particular cryptochirid taxa along the specialist–generalist continuum, however, remains much obscure until precise species-level diversity can be recognized. This highlights the imperativeness of investigations in species diversity in a refined, integrated approach for some twofold "cryptic" cryptochirids.

Data availability statement

The data presented in the study are deposited in the NCBI Genbank, with accession numbers indicated in Table 1.

Author contributions

KJHW, Y-FT, J-WQ, and BKKC conducted field sampling. J-WQ provided logistic support. Y-FT and KJHW performed molecular analyses. KJHW wrote early drafts of the MS. All authors contributed to the article and approved the submitted version.

Acknowledgments

We thank P.-C. Tsai (Academia Sinica), J. X. Xie, and Y. H. Yeung (HKBU) for assistance in field collection and Dr. Y. Nozawa (Academia Sinica) for advice in coral identification. BKKC is supported by the Academia Sinica Senior Investigator Award and National Science and

Technology Council, Taiwan (109-2621-B-001 -003 -MY3). The cryptochirid crabs were collected while implementing projects supported by Environment and Conservation Fund, Hong Kong (2011-08, 2015-84, 2017-03). KJHW is supported by postgraduate studentship in Institute of Ecology and Evolutionary Biology, National Taiwan University, Taiwan. We are grateful to reviewers for their time and effort in providing much helpful advice on the manuscript.

Conflict of interest

The authors declare that the research was conducted in the absence of any commercial or financial relationships that could be construed as a potential conflict of interest.

Publisher's note

Supplementary material

The Supplementary Material for this article can be found online at: https://www.frontiersin.org/articles/10.3389/fmars.2022.1003321/full#supplementary-material

APPENDIX 1
List of non-cryptochirid taxa mentioned in the text, with respective authorities.

References

Abelson, A., Galil, B. S., and Loya, Y. (1991). Skeletal modifications in stony corals caused by indwelling crabs: hydrodynamical advantages for crab feeding. *Symbiosis* 10, 233–248.

Arrigoni, R., Stefani, F., Pichon, M., Galli, P., and Benzoni, F. (2012). Molecular phylogeny of the robust clade (Faviidae, Mussidae, Merulinidae, and Pectiniidae): An Indian ocean perspective. *Mol. Phyl. Evol.* 65, 183–193. doi: 10.1016/j.ympev.2012.06.001

Bähr, S., Johnson, M. L., Berumen, M. L., Hardenstine, R. S., Rich, W. A., and van der Meij, S. E. T. (2021). Morphology and reproduction in the *Hapalocarcinus marsupialis* Stimpson, 1859 species complex (Decapoda: Brachyura: Cryptochiridae). *J. Crust. Biol.* 41 (3), 1–15. doi: 10.1093/jcbiol/ruab052

Benzoni, F., Arrigoni, R., Stefani, F., and Pichon, M. (2011). Phylogeny of the coral genus *Plesiastrea* (Cnidaria, scleractinia). *Contrib. Zool.* 80 (4), 231–249. doi: 10.1163/18759866-08004002

Bickford, D., Lohman, D. J., Sodhi, N. S., Ng, P. K. L., Meier, R., Winker, K., et al. (2007). Cryptic species as a window on diversity and conservation. *Trends Ecol. Evol.* 22 (3), 148–155. doi: 10.1016/j.tree.2006.11.004

Borradaile, L. A. (1902). "Marine crustaceans. III. the Xanthidae and some other crabs," in *The fauna and geography of the Maldive and Laccadive Archipelagoes, being the account of the work carried on and of the collections made by an expedition during the years 1899 and 1900*, vol. Vol. 1 . Ed. J. S. Gardiner (Cambridge: Cambridge University), 237–271.

Bucklin, A., Steinke, D., and Blanco-Bercial, L. (2011). DNA Barcoding of marine metazoa. *Ann. Rev. Mar. Sci.* 3, 471–508. doi: 10.1111/j.1096-3642.2012.00855.x

Castro, P. (1976). Brachyuran crabs symbiotic with scleractinian corals. *Mar. Biol.* 46, 237–245.

Castro, P. (2011). Catalog of the Anomuran and Brachyuran crabs (Crustacea: Decapoda: Anomura, Brachyura) of the Hawaiian Islands. *Zootaxa* 2947, 1–154. doi: 10.11646/zootaxa.2947.1.1

Castro, P. (2015). "Symbiotic Brachyura," in *Decapoda: Brachyura, treatise on zoology – anatomy, taxonomy, biology*, vol. vol. 9C-I . Eds. P. Castro, P. Davie, D. Guinot, R. Schram and J. C. von Vaupel Klein (Leiden: Boston: Brill), 543–581. doi: 10.1163/9789004190832_012

Chan, A. L. K., Chan, K. K., Choi, C. L. S., McCorry, D., Lee, M. W., and Ang, P. Jr (2005). *Field guide to hard corals of Hong Kong* (Hong Kong: Friends of the Country Parks, Cosmos Books Ltd).

Cheang, C.-C., Chow, C.-F., and Fok, L. (2017). "The unconventional learning experience of students – becoming a courier of marine stewardship," in *Emerging practices in scholarship of learning and teaching in a digital era*. Eds. S. C. Kong, T. L. Wong, M. Yang, C. F. Chow and K. H. Tse (Singapore: Springer Nature Singapore Pte Ltd), 151–170. doi: 10.1007/978-981-10-3344-5_10

Chilton, C. (1911). The Crustacea of the Kermadec Islands. *Trans. Proc. New Z. Inst.* 43, 544–573.

Chu, K. H., Schubart, C. D., Shih, H.-T., and Tsang, L. M. (2015). "Genetic diversity and evolution of Brachyura," in *Decapoda: Brachyura, treatise on zoology – anatomy, taxonomy, biology*, vol. vol. 9C-II . Eds. P. Castro, P. Davie, D. Guinot, F. R. Schram and J. C. von Vaupel Klein (Leiden: Boston: Brill), 755–820. doi: 10.1163/9789004190832_016

Crandall, K. A., and Fitzpatrick, J. F.Jr (1996). Crayfish molecular systematics: Using a combination of procedures to estimate phylogeny. *Syst. Biol.* 45, 1–26. doi: 10.1093/sysbio/45.1.1

Crossland, C. J., Hatcher, B. G., and Smith, S. V. (1991). Role of coral reefs in global ocean production. *Coral Reefs* 10, 55–64.

Dai, C.-F., and Cheng, Y.-R. (2020). *Corals of Taiwan Vol. 1: Scleractinia Fauna* (Taipei: Owl Publishing House Co. Ltd).

Dai, C.-f., and Horng, S. (2009). *Scleractinia Fauna of Taiwan Vol. II. The Robust Group* (Taipei: National Taiwan University).

Davie, P. J. F. (2002). "Crustacea: Malacostraca: Eucarida (part 2): Decapoda — Anomura, Brachyura," in *Zoological catalogue of Australia*, vol. Vol. 19.3B . Eds. A. Wells and W. W. K. Houston (Melbourne: CSIRO Publishing), 1–641.

Davie, P. J. F., Guinot, D., and Ng, P. K. L. (2015). *Anatomy and functional morphology of Brachyura. in Decapoda: Brachyura, treatise on zoology – anatomy, taxonomy, biology* Vol. vol. 9C-I. Eds. P. Castro, P. Davie, D. Guinot, F. R. Schram and J. C. von Vaupel Klein (Leiden: Boston: Brill), 11–163. doi: 10.1163/9789004190832_004

Davie, P. J. F., Shih, H.-T., and Chan, B. K. K. (2010). "A new species of *Mictyris* (Decapoda, Brachyura, mictyridae) from the Ryukyu Islands, Japan," in *Studies on Brachyura: A homage to Danièle Guinot. Crustacean Monographs*, Vol. 11 . Eds. P. Castro, P. J. F. Davie, P. K. L. Ng and B. Richer de Forges (Leiden: Brill), 83–105. doi: 10.1163/ej.9789004170865.i-366.61

De Gier, W., and Becker, C. (2020). A review of the ecomorphology of pinnotherinae pea crabs (Brachyura: Pinnotheridae), with an updated list of symbiont-host associations. *Diversity* 12 (431). doi: 10.3390/d12110431

De Grave, S., Dworschak, P. C., Low, M. E. Y., and Ng, P. K. L. (2022). The Decapoda described by the Austrian carcinologist Camill Heller (1823–1917): checklist, dates of publication and bibliography. *Ann. Naturhist. Mus. Wien B* 124, 265–299.

Edmondson, C. H. (1925). Marine zoology of tropical Central Pacific. Crustacea. *Bull. Bernice P. Bishop Mus.* 27, 3–62.

Edmondson, C. H. (1933). *Cryptochirus* of the Central Pacific. *Bernice P. Bishop Mus. Occ. Pap.* 10 (5), 1–23.

Feller, K. D., Cronin, T. W., Ahyong, S. T., and Porter, M. L. (2013). Morphological and molecular description of the late-stage larvae of *Alima* Leach, 1817 (Crustacea: Stomatopoda) from Lizard Island, Australia. *Zootaxa* 3722, 22–32. doi: 10.11646/zootaxa.3722.1.2

Fernandes, G. W., Carneiro, M. A. A., and Isaias, R. M. S. (2011). "Gall-inducing insects: from anatomy to biodiversity," in *Insect bioecology and nutrition for integrated pest management*. Eds. A. R. Panizzi and J. R. P. Parra (Boca Raton: CRC Press), 369–395.

Fisher, R., O'Leary, R. A., Low-Choy, S., Mengersen, K., Knowlton, N., Brainard, R. E., et al. (2015). Species richness on coral reefs and the pursuit of convergent global estimates. *Curr. Biol.* 25, 500–505. doi: 10.1016/j.cub.2014.12.022

Fize, A., and Serène, R. (1956a). Note préliminaire sur huit espèces nouvelles, dont une d'un genre nouveau, d'Hapalocarcinidae. *Bull. Soc Zool. France* 80 (5–6), 375–378.

Fize, A., and Serène, R. (1956b). Note préliminaire sur quatre espèces nouvelles d'Hapalocarcinidés avec quelques remarques au sujet du *Cryptochirus rugosus* Edmondson. *Bull. Soc Zool. France* 80 (5–6), 379–382.

Fize, A., and Serène, R. (1957). Les Hapalocarcinidés du Việt-nam. *Arch. Mus. Natl. Hist. nat. Paris Sèp. Sér.* 5. i-xiii + 1–202, pls. I–XVIII.

Folmer, O., Black, M., Hoeh, W., Lutz, R., and Vrijenhoek, R. (1994). DNA Primers for amplification of mitochondrial cytochrome c oxidase subunit I from diverse metazoan invertebrates. *Mol. Mar. Biol. Biotechnol.* 3, 294–299.

Fukami, H., Chen, C. A., Budd, A. F., Collins, A., Wallace, C., Chuang, Y.-Y., et al. (2008). Mitochondrial and nuclear genes suggest that stony corals are monophyletic but most families of stony corals are not (Order scleractinia, class anthozoa, phylum cnidaria). *PLoS One* 3 (9), e3222. doi: 10.1371/journal.pone.0003222

García-Hernández, J. E., de Gier, W., van Moorsel, G. W. N. M., and Hoeksema, B. W. (2020). The scleractinian *Agaricia undata* as a new host for the coral-gall crab *Opecarcinus hypostegus* at Bonaire, Southern Caribbean. *Symbiosis* 81, 303–311. doi: 10.1007/s13199-020-00706-8

Goodkin, N. F., Switzer, A. D., McCorry, D., DeVantier, L., True, J. D., Hughen, K. A., et al. (2011). Coral communities of Hong Kong: Long-lived corals in a marginal reef environment. *Mar. Ecol. Prog. Ser.* 426, 185–196. doi: 10.3354/meps09019

Gore, R. H., Scotto, L. E., and Reed, J. K. (1983). Early larval stages of the Indo-Pacific coral gall-forming crab *Hapalocarcinus marsupialis* Stimpson 1859 (Brachyura, Hapalocarcinidae) cultured in the laboratory. *Crustaceana* 44, 141–150. doi: 10.1163/156854083X00767

Guinot, D., Tavares, M., and Castro, P. (2013). Significance of the sexual openings and supplementary structures on the phylogeny of Brachyuran crabs (Crustacea, Decapoda, Brachyura), with new nomina for higher-ranked podotreme taxa. *Zootaxa* 3665 (1), 1–414. doi: 10.11646/zootaxa.3665.1.1

Heller, C. (1860). Beiträge zur crustaceen-fauna des Rothen Meeres. Erster TheiI. *Sitz. Math.-Nat. Kl. Kai. Akad. Wiss. Wien* 43, 297–374.

Heller, C. (1861). Synopsis der im rothen meere vorkommenden crustaceen. *Verh. Zool.Bot. Gesell. Wien* 11, 3–32.

Hiro, F. (1937). Studies on the animals inhabiting reef corals. I. *Hapalocarcinus Cryptochirus. Palao Trop. Biol. Stat. Stud.* 1, 137–154.

Hoeksema, B. W. (2017). The hidden biodiversity of tropical coral reefs. *Biodiversity*. doi: 10.1080/14888386.2017.1307787

Hoeksema, B. W., and Cairns, S. (2022) *World list of scleractinia*. Available at: http://www.marinespecies.org/scleractinia/ (Accessed 2 Sep 2022).

Hoeksema, B. W., van Beusekom, M., ten Hove, H. A., Ivanenko, V. N., van der Meij, S. E. T., and van Moorel, G. W. N. M. (2017). *Helioseris cucullata* as a host coral at St. Eustatius, Dutch Caribbean. *Mar. Biodiv.* 47, 71–78. doi: 10.1007/s12526-016-0599-6

Hoeksema, B. W., van der Meij, S. E. T., and Fransen, C. H. J. M. (2012). The mushroom coral as a habitat. *J. Mar. Biol. Assoc. U. K.* 92 (4), 647–663. doi: 10.1017/S0025315411001445

Huang, D., Benzoni, F., Fukami, H., Knowlton, N., Smith, N. D., and Budd, A. F. (2014). Taxonomic classification of the reef coral Families Merulinidae, Montastraeidae, and Diploastraeidae (Cnidaria: Anthozoa: Scleractinia). *Zool. J. Linn. Soc* 171, 277–355. doi: 10.1111/zoj.12140

Juszkiewicz, D. J., White, N. E., Stolarski, J., Benzoni, F., Arrigoni, R., Hoeksema, B. W., et al. (2022). Phylogeography of recent *Plesiastrea* (Scleractinia: Plesiastreidae) based on an integrated taxonomic approach. *Mol. Phyl. Evol.* 172, 107469. doi: 10.1016/j.ympev.2022.107469

Kobayashi, G., Itoh, H., Fukuda, H., and Kojima, S. (2021). The complete mitochondrial genome of the sand bubbler crab *Scopimera globosa* and its phylogenetic position. *Genomics* 113, 831–839. doi: 10.1016/j.ygeno.2020.10.014

Kropp, R. K. (1988a). The status of *Cryptochirus coralliodytes* Heller and *Lithoscapthus paradoxus* Milne Edwards (Brachyura: Cryptochiridae). *Proc. Biol. Soc Washington* 101, 872–882.

Kropp, R. K. (1988b). The status of *Cryptochirus hongkongensis* Shen, 1936 (Brachyura: Cryptochiridae). *Proc. Biol. Soc Washington* 101 (4), 866–871.

Kropp, R. K. (1989). A revision of the Pacific species of gall crabs, genus *Opecarcinus* (Crustacea: Cryptochiridae). *Bull. Mar. Sci.* 45, 98–129.

Kropp, R. K. (1990). Revision of the genera of gall crabs (Crustacea: Cryptochiridae) occurring in the Pacific Ocean. *Pacific Sci.* 44, 417–448.

Kropp, R. K. (1994). The gall crabs (Crustacea: Decapoda: Brachyura: Cryptochiridae) of the Rumphius Expeditions revisited, with descriptions of three new species. *Raffles Bull. Zool* 42, 521–538.

Kropp, R. K. (1995). *Lithoscaptus pardalotus*, a new species of coral-dwelling gall crab (Crustacea: Brachyura: Cryptochiridae) from Belau. *Proc. Biol. Soc. Washington* 108, 637–642.

Kropp, R. K., and Manning, R. B. (1987). The Atlantic gall crabs, Family Cryptochiridae (Crustacea: Decapoda: Brachyura). *Smithsonian Contrib. Zool.* 462, 1–21.

Kumar, S., Stecher, G., Li, M., Knyaz, C., and Tamura, K. (2018). MEGA X: molecular evolutionary genetics analysis across computing platforms. *Mol. Biol. Evol.* 35, 1547–1549. doi: 10.1093/molbev/msy096

Lajus, D., Sukhikh, N., and Alekseev, V. (2015). Cryptic or pseudocryptic: Can morphological methods inform copepod taxonomy? an analysis of publications and a case study of the *Eurytemora affinis* species complex. *Ecol. Evol.* 5, 2374–2385.

McNeill, F. A. (1968). Crustacea, Decapoda & Stomatopoda. *Great Barrier Reef Exp. 1928–29 Sci. Rep.* 7 (1), 1–98.

Milne-Edwards, A. (1862). "Faune carcinologique de l'île de la réunion," in *Notes sur l'île de la réunion*, vol. 1–16 . Ed. L. Maillard (Paris).

Mora, C., Tittensor, D. P., Adl, S., Simpson, A. G. B., and Worm, B. (2011). How many species are there on earth and in the ocean? *PLoS Biol.* 9 (8), e1001127. doi: 10.1371/journal.pbio.1001127

Morton, B. (1989). Pollution of the coastal waters of Hong Kong. *Mar. Pollut. Bull.* 20 (7), 310–318. doi: 10.1016/0025-326X(89)90153-7

Morton, B., Williams, G. A., and Lee, S. Y. (1996). "The benthic marine ecology of Hong Kong: A dwindling heritage?," in *Coastal infrastructure development in Hong Kong. A review. Proceedings of the symposium on hydraulics of Hong Kong waters held in Hong Kong on 28–29 November 1995* (Hong Kong: Civil Engineering Department, Hong Kong Government), 233–267.

Ng, P. K. L., and Davie, P. J. F. (2002). A checklist of the Brachyuran crabs of phuket and western Thailand. *Phuket Mar. Biol. Cent. Sp. Publ.* 23 (2), 369–384.

Ng, P. K. L., Guinot, D., and Davie, P. J. F. (2008). Systema brachyurorum: Part i. an annotated checklist of extant Brachyuran crabs of the world. *Raffles Bull. Zool. Supp.* 17, 1–286.

Paulay, G., Kropp, R., Ng, P. K. L., and Eldredge, L. G. (2003). The crustaceans and pycnogonids of the Mariana Islands. *Micronesica* 35–36, 456–513.

Paul'son, O. (1875). Studies on Crustacea of the Red Sea with notes regarding other seas. Part I. *Podophthalmata and Edriophthalmata (Cumacea)* (Kiev: S.V. Kul'zhenko), 1–144.

Potts, F. A. (1915). *Hapalocarcinus*, the gall-forming crab, with some notes on the related genus *Cryptochirus*. *Pap. Tortugas Lab. Carnegie Inst. Washington* 833–69.

Poupin, J. (1996). Crustacea Decapoda of French Polynesia (Astacidea, Palinuridea, Anomura, Brachyura). *Atoll Res. Bull.* 442, 1–114.

Poupin, J. (2005). *Systématique et ecologie des crustacés décapodes et stomatopodes de polynésie française* (France: l'Institut de Recherche de l'Ecole Navale, Université de Perpignan).

Ragionieri, L., Fratini, S., and Schubart, C. D. (2012). Revision of the *Neosarmatium meinerti* species complex (Decapoda: Brachyura: Sesarmidae), with descriptions of three pseudocryptic Indo-West Pacific species. *Raffles Bull. Zool.* 60 (1), 71–87.

Reaka-Kudla, M. L. (1997). "The global diversity of coral reefs: A comparison with rainforests," in *Biodiversity II: Understanding and protecting our natural resources*. Eds. M. L. Reaka-Kudla, D. E. Wilson and E. O. Wilson (Washington D. C: Joseph Henry / National Academy Press), 83–108.

Richer de Forges, B., and Ng, P. K. L. (2006). "The Brachyura of new Caledonia," in *Compendium of marine species from new Caledonia*. Eds. C. Payri and B. Richer de Forges (Nouméa: IRD), 273–289.

Richters, F. (1880). "Decapoda," in *Beiträge zur meeresfauna der insel Mauritius und der seychellen*. Eds. K. Möbius, F. Richters, E. von Martens nach Sammlungen and K. Möbius (Berlin: Verlag der Gutmann'schen Buchhandlung), 139–178.

Ross, D. M. (1983). "Symbiotic relations," in *The biology of the Crustacea*, vol. vol. 7 . Ed. D. Bliss (New York: Academic Press), 163–212.

Scott, P. J. B. (1984). *The corals of Hong Kong* (Hong Kong: Hong Kong University Press).

Scott, P. J. B., and Cope, M. (1982). "The distribution of scleractinian corals at six sites within Tolo Harbour and Channel," in *Proceedings of the first international marine biological workshop: The marine flora and fauna of Hong Kong and Southern China, Hong kon*. Eds. B. Morton and C. K. Tseng (Hong Kong: Hong Kong University Press), 587–594.

Scott, P. J. B., and Cope, M. (1990). "Tolo revisited: A survey of the corals in Tolo Harbour and Channel six years and half a million people later," in *The marine flora and fauna of Hong Kong and Southern china. proceedings of the second international marine biological workshop: The marine flora and fauna of Hong Kong and Southern China, Hong Kong 1986*. Ed. B. Morton (Hong Kong: Hong Kong University Press), 1203–1220.

Semper, C. (1881). *Animal life as affected by the natural conditions of existence* (New York: D. Appleton and company).

Serène, R. (1968). "Note sur la taxonomie et la distribution geographique des hapalocarcinidae (Decapoda-Brachyura)," in *Proceedings of the symposium on Crustacea held at ernakulam from January 12 to 15, 1965*, vol. volume 1 . Ed. N. K. Pillai (Bangalore, India: Marine Biological Association of India), 395–398.

Shen, C.-J. (1936). Notes on the Family Hapalocarcinidae (coral-infesting crabs) with description of two new species. *Hong Kong Nat. Suppl.* 5, 21–26.

Shen, C.-J. (1940). The Brachyuran fauna of Hong Kong. *J. Hong Kong Fish. Res. Stat.* 1 (2), 211–242.

Shih, H.-T., Fang, S.-H., and Ng, P. K. L. (2007). Phylogeny of the freshwater crab genus *Somanniathelphusa* Bott (Decapoda: Parathelphusidae) from Taiwan and the coastal regions of China, with notes on their biogeography. *Invert. Syst.* 21, 29–37. doi: 10.1071/IS06007

Shih, H.-T., Hsu, P.-Y., Shahdadi, A., Schubart, C. D., and Li, J.-J. (2019). The synonymy of the supratidal crab species *Parasesarma cognatum* Rahayu & Li, 2013 with *P. liho* Koller, Liu & Schubart, 2010 (Decapoda: Brachyura: Sesarmidae) based on morphological and molecular evidence, with a note on *P. paucitorum* Rahayu & Ng, 2009. *Zool. Stud.* 58, 21. doi: 10.6620/ZS.2019.58-21

Shih, H.-T., Naruse, T., and Ng, P. K. L. (2010). *Uca jocelynae* sp. nov., a new species of fiddler crab (Crustacea: Brachyura: Ocypodidae) from the Western Pacific. *Zootaxa* 2337, 47–62. doi: 10.11646/zootaxa.2337.1.4

Shih, H.-T., Ng, P. K. L., Wong, K. J. H., and Chan, B. K. K. (2012). *Gelasimus splendidus* Stimpson 1858 (Crustacea: Brachyura: Ocypodidae), a valid species of fiddler crab from the northern South China Sea and Taiwan Strait. *Zootaxa* 3490, 30–47. doi: 10.11646/zootaxa.3490.1.2

Shih, H.-T., and Suzuki, H. (2008). Taxonomy, phylogeny, and biogeography of the endemic mudflat crab *Helice*/*Chasmagnathus* complex (Crustacea: Brachyura: Varunidae) from East Asia. *Zool. Stud.* 47 (1), 114–125.

Simon-Blecher, N., and Achituv, Y. (1997). Relationship between the coral pit crab *Cryptochirus coralliodytes* Heller and its host coral. *J. Exp. Mar. Biol. Ecol.* 215, 93–102. doi: 10.1016/S0022-0981(97)00002-6

Sun, S., Jiang, W., Yuan, Z., and Sha, Z. (2022). Mitogenomes provide insights into the evolution of thoracotremata (Brachyura: EuBrachyura). *Front. Mar. Sci.* doi: 10.3389/fmars.2022.848203Takeda

Takeda, M., and Tamura, Y. (1980). Coral-inhabiting crabs of the Family Cryptochiridae from Japan V. Genus *Cryptochirus*. *Res. Crust.* 10, 45–56.

Takeda, M., and Tamura, Y. (1981a). Coral-inhabiting crabs of the Family Cryptochiridae from Japan VII. Genus. *Favicola*. *Res. Crust.* 11, 41–50.

Takeda, M., and Tamura, Y. (1981b). Coral-inhabiting crabs of the Family Hapalocarcinidae from Japan VIII. Genus *Pseudocryptochirus* two new genera. *Bull. Biogeog. Soc Japan* 36 (3), 13–27.

Takeda, M., and Tamura, Y. (1983). Coral-inhabiting crabs of the Family Hapalocarcinidae from Japan. A small collection made at Kushimoto and Koza, Kii Peninsula. *Bull. Natl. Sci. Mus. Tokyo Ser. A Zool.* 9, 1–12.

Takeda, M., and Tamura, Y. (1985). Coral-inhabiting crabs of the Family Hapalocarcinidae from Japan X. Collections from Hachijo Island in the Izu Islands. *Bull. Natl. Sci. Mus. Tokyo Ser. A Zool.* 11, 99–108.

Tam, T.-W., and Ang, P. O.Jr (2008). Repeated physical disturbances and the stability of sub-tropical coral communities in Hong Kong, China. *Aq. Cons. Mar. Freshwat. Ecosyst.* 18, 1105–1024. doi: 10.1002/aqc.922

Tamura, K., Stecher, G., and Kumar, S. (2021). MEGA11: Molecular evolutionary genetics analysis version 11. *Mol. Biol. Evol.* 38, 3022–3027. doi: 10.1093/molbev/msab120

Utinomi, H. (1944). Studies on the animals inhabiting reef corals. III. A revision of the Family Hapalocarcinidae (Brachyura) with some remarks on their morphological peculiarities. *Palao Trop. Biol. Stat. Stud.* 2, 687–731.

van der Meij, S. E. T. (2012). Host preferences, colour patterns and distribution records of *Pseudocryptochirus viridis* Hiro 1938 (Decapoda, cryptochiridae). *Crustaceana* 85, 769–777. doi: 10.1163/156854012X650223

van der Meij, S. E. T. (2014). A new species of *Opecarcinus* Kropp & Manning, 1987 (Crustacea: Brachyura: Cryptochiridae) associated with the stony corals *Pavona clavus* (Dana, 1846) and *P. bipartita* Nemenzo, 1980 (Scleractinia: Agariciidae). *Zootaxa* 3869 (1), 44–52. doi: 10.11646/zootaxa.3869.1.4

van der Meij, S. E. T. (2015a). Host relations and DNA reveal a cryptic gall crab species (Crustacea: Decapoda: Cryptochiridae) associated with mushroom corals (Scleractinia: Fungiidae). *Contrib. Zool.* 84 (1), 39–57. doi: 10.1163/18759866-08401004

van der Meij, S. E. T. (2015b). A new gall crab species (Brachyura, cryptochiridae) associated with the free-living coral *Trachyphyllia geoffroyi* (Scleractinia, merulinidae). *Zookeys* 500, 61–72. doi: 10.3897/zookeys.500.9244

van der Meij, S. E. T. (2017). The coral genus *Caulastraea* Dana, 1846 (Scleractinia, Merulinidae) as a new host for gall crabs (Decapoda, cryptochiridae), with the description of *Lithoscaptus tuerkayi* sp nov. *Crustaceana* 90 (7-10), 1027–1038. doi: 10.1163/15685403-00003607

van der Meij, S. E. T., Fransen, C. H. J. M., Pasman, L. R., and Hoeksema, B. W. (2015). Phylogenetic ecology of gall crabs (Cryptochiridae) as associates of mushroom corals (Fungiidae). *Ecol. Evol.* 5 (24), 5770–5780. doi: 10.1002/ece3.1808

van der Meij, S. E. T., and Nieman, A. M. (2016). Old and new DNA unweave the phylogenetic position of the eastern Atlantic gall crab *Detocarcinus balssi* (Monod, 1956) (Decapoda: Cryptochiridae). *J. Zool. Syst. Evol. Res.* 54, 189–196. doi: 10.1111/jzs.12130

van der Meij, S. E. T., and Reijnen, B. T. (2014). The curious case of *Neotroglocarcinus dawydoffi* (Decapoda, cryptochiridae): Unforeseen biogeographic patterns resulting from isolation. *Syst. Biodiv.* 12, 503–512. doi: 10.1080/14772000.2014.946979

Vehof, J., van der Meij, S. E. T., Türkay, M., and Becker, C. (2014). Female reproductive morphology of coral-inhabiting gall crabs (Crustacea: Decapoda: Brachyura: Cryptochiridae). *Acta Zool. Stockholm* 97 (1), 117–126. doi: 10.1111/azo.12111

Veron, J. E. N. (1982). "Hermatypic scleractinia of Hong Kong — an annotated list of species," in *The marine flora and fauna of Hong Kong and Southern China proceedings of the first international marine biological workshop: The marine flora and fauna of Hong Kong and Southern China, Hong Kong*. Eds. B. Morton and C. K. Tseng (Hong Kong: Hong Kong University Press), 111–125.

Veron, J. E. N. (2000). *Corals of the world* (Australian Institute of Marine Science and CRR Ald Pty Ltd).

Verrill, A. E. (1866). Synopsis of the polyps and corals of the north Pacific exploring expedition, under commodore c. ringgold and Capt. John Rodgers, U. S. N., from 1853 to 1856. collected by Dr. Wm. Stimpson, naturalist to the expedition. with descriptions of some additional species from the west coast of North America. part III. Madreporaria. *Proc. Essex Inst. Salem* 5 (3), 17–50.

Wei, T.-P., Hwang, J.-S., Peng, S.-H., Chen, H.-C., and Lee, Y.-C. (2016). Genetic diversification of the gall crab, *Hapalocarcinus marsupialis* (Crustacea: Decapoda: Cryptochiridae), related to their host corals (Scleractinia: Pocilloporidae). *J. Fish. Soc Taiwan* 43, 135–144.

Wei, T.-P., Hwang, J.-S., Tsai, M.-L., and Fang, L.-S. (2006). New records of gall crabs (Decapoda, cryptochiridae) from Orchid Island, Taiwan, northwestern Pacific. *Crustaceana* 78 (9), 1063–1077. doi: 10.1163/156854005775361025

Wong, K. J. H., Shih, H.-T., and Chan, B. K. K. (2012). The ghost crab *Ocypode mortoni* George 1982, (Crustacea: Decapoda: Ocypodidae): redescription, distribution at its type locality, and the phylogeny of East Asian *Ocypode* species. *Zootaxa* 3550, 71–87. doi: 10.11646/zootaxa.3550.1

Wong, K. T., Chui, A. P. Y., Lam, E. K. Y., and Ang, P.Jr (2018). A 30-year monitoring of changes in coral community structure following anthropogenic disturbances in Tolo Harbour and Channel, Hong Kong. *Mar. Pollut. Bull.* 133, 900–910. doi: 10.1016/j.marpolbul.2018.06.049

Wong, K. T., Tsang, R. H. L., and Ang, P.Jr (2015). Did borers make corals more susceptible to a catastrophic disease outbreak in Hong Kong? *Mar. Biodiv.* 46, 325–326. doi: 10.1007/s12526-015-0382-0

Xie, J. Y., Wong, J. C., Dumont, C. P., Goodkin, N., and Qiu, J. W. (2016). Borehole density on the surface of living *Porites* corals as an indicator of sedimentation in Hong Kong. *Mar. Pollut. Bull.* 108, 87–93. doi: 10.1016/j.marpolbul.2016.04.055

Xu, T., Bravo, H., Paulay, G., and van der Meij, S. E. T. (2021). Diversity and distribution of gall crabs (Brachyura: Cryptochiride: *Opecarcinus*) associated with agaridiidae corals. *Coral Reefs*. doi: 10.1007/s00338-021-02163-1

Yang, S., Chen, H., and Jiang, W. (2008). "Infraorder Brachyura Latreill," in *Checklist of marine biota of China seas*. Ed. R. Liu (Beijing: Science Press), 761–810.

Yeo, D. C. J., Shih, H.-T., Meier, R., and Ng, P. K. L. (2007). Phylogeny and biogeography of the freshwater crab genus *Johora* (Crustacea: Brachyura: Potamidae) from the Malay Peninsula, and the origins of its insular fauna. *Zool. Scrip.* 36 (3), 255–269. doi: 10.1111/j.1463-6409.2007.00276.x

Yeung, Y. H., Xie, J. Y., Kwok, C. K., Kei, K., Ang, P.Jr., Chan, L. L., et al. (2021a). Hong Kong's subtropical scleractinian coral communities: Baseline, environmental drivers and management implications. *Mar. Pollut. Bull.* 167, 112289. doi: 10.1016/j.marpolbul.2021.112289

Yeung, Y. H., Xie, J. X., Lai, V. C. S., and Qiu, J. W. (2021b). Can portunid crabs protect massive coral against the attack by long-spined sea urchins? *Reg. Stud. Mar. Sci.* 38, 101374. doi: 10.1016/j.rsma.2020.101374

Yu, M.-C., Kolbasov, G. A., Høeg, J. T., and Chan, B. K. K. (2019). Crustacean-sponge symbiosis: collecting and maintaining sponge-inhabiting barnacles (Cirripedia: Thoracica: Acastinae) for studies on host specificity and larval biology. *J. Crust. Biol.* 39 (4), 522–532. doi: 10.1093/jcbiol/ruz025

Zhang, Y., Ip, J. C., Xie, J. Y., Yeung, Y. H., Sun, Y., and Qiu, J. W. (2022). Host-symbiont transcriptomic changes during natural bleaching and recovery in the leaf coral *Pavona decussata*. *Sci. Total Environ.* 806, 150656. doi: 10.1016/j.scitotenv.2021.150656

Zou, R., Li, C., Zhou, J., Xu, Z., and Dai, C.-F. (2008). "Scleractinia," in *Checklist of marine biota of China seas*. Ed. R. Liu (Beijing: Science Press), 305–325.